Larhyss Journal, ISSN 1112-3680, n°63, Sep 2025, pp. 7-54

CRESTLESS CONTRACTED V-NOTCH WEIR FOR FLOW MEASUREMENT IN TRIANGULAR OPEN CHANNELS

***ACHOUR B.*[1*], *AMARA L.*[2], *KULKARNI K.H.*[3]**

[1] Professor, Research Laboratory in Subterranean and Surface Hydraulics (LARHYSS), University of Biskra, PO Box 145 RP, Biskra, Algeria
[2] Associate Professor, Department of Civil Engineering and Hydraulics, Faculty of Science and Technology, University of Jijel, PO Box 98, Ouled Aissa, Jijel, Algeria
[3] Associate Professor, Department of Civil Engineering, Dr Vishwanath Karad MIT World Peace University, 411038, Pune, India

(*) bachir.achour@larhyss.net

Research Article – Available at http://larhyss.net/ojs/index.php/larhyss/index
Received January 21, 2025, Received in revised form September 2, 2025, Accepted September 4, 2025

ABSTRACT

Accurate flow measurement in triangular open channels remains a significant challenge in hydraulic engineering, primarily due to the lack of simple and cost-effective devices tailored to these geometries. Existing solutions, such as non-intrusive flow measurement devices including laser Doppler velocimeter, ultrasonic, and electromagnetic flow meters, although highly accurate, are prohibitively expensive and require specialized maintenance and calibration. Furthermore, conventional weirs and flumes, including triangular, rectangular and trapezoidal designs, are ill-suited for triangular channel profiles, limiting their practical applicability in such contexts.

In response to this gap, the present study introduces a novel and economical approach for measuring discharge in triangular open channels, utilizing a contracted V-notch weir installed at the downstream end of the channel. Distinguished by its simplicity of construction and ease of implementation, the proposed device eliminates the need for a crest height, facilitating self-cleaning operation and minimizing maintenance demands. The study formulates a rigorous theoretical framework for the discharge coefficient (C_d), explicitly expressed as a function of the dimensionless section reduction ratio ($\zeta = m_2 / m_1 = b / T$), where m_1 and m_2 are the side slopes of the approach channel and V-notch, respectively, and b and T are their corresponding top widths. The discharge coefficient derived from this relationship is shown to be invariant with respect to upstream flow depth h_1, simplifying its practical use.

The validity of the theoretical formulation is assessed through an extensive experimental program involving nine different V-notch configurations, with section reduction ratios varying from 0.35 to 0.50. This carefully selected range ensures an optimal compromise

between sustaining critical flow conditions within the V-notch and avoiding adverse surface tension effects, thereby safeguarding the precision and broader applicability of the proposed methodology.

A total of 2,879 experimental C_d values were collected under diverse flow conditions. The experimental discharge coefficients demonstrated remarkable agreement with the theoretical predictions, with a maximum deviation not exceeding 0.015%. This confirms the accuracy, robustness, and reliability of the proposed theoretical discharge coefficient relationship and its suitability for practical applications.

The findings of this study offer a simple, inexpensive, and highly accurate alternative for flow measurement in triangular open approach channels, making the crestless contracted V-notch a practical solution for use in irrigation canals, water distribution networks, and field monitoring programs.

Future research should explore the adaptation of this methodology to other non-standard channel geometries and flow conditions.

Keywords: V-notch weir, Triangular open channels, Flow measurement, Discharge coefficient, Section reduction ratio.

INTRODUCTION

The accurate measurement of flow in open channels and pipelines has long been a fundamental challenge in the field of hydraulics, driving the evolution of gauging techniques that integrate theoretical precision with practical feasibility. These methodologies are designed to ensure the reliable quantification of discharge, a critical parameter in water resource management, irrigation infrastructure, and hydraulic engineering applications.

Among the wide range of flow measurement devices, weirs have established themselves as fundamental tools due to their capacity to leverage the principles of free-spilling flow. These hydraulic structures, distinguished by their unique geometric designs, induce controlled flow conditions that enable precise discharge estimation. Weirs are classified based on their crest profiles, which may consist of thin vertical plates or incorporate notches of varying shapes, including V-notch, rectangular, trapezoidal, or parabolic configurations, each tailored to specific measurement needs. The V-notch weir, commonly referred to as the Thomson weir, is particularly well-regarded for its heightened sensitivity to low flow rates. It is widely recognized for its superior accuracy in measuring upstream flow depth, as its triangular configuration inherently enhances the precision of depth readings across a broad range of flow conditions. This attribute makes the V-notch weir an optimal choice for applications requiring exceptional accuracy in discharge calculations, particularly at both low and high flow rates.

In contrast, sharp-crested rectangular weirs, despite their historical significance, demonstrate reduced accuracy when measuring low flow conditions. This limitation stems primarily from their susceptibility to lateral contraction effects, which alter the flow

profile and introduce measurement discrepancies. Such distortions can significantly impact discharge calculations, leading to deviations from theoretical predictions. This challenge has been extensively documented in foundational research, including the works of Bazin (1898), SIA (1926), Kindsvater and Carter (1957), De Coursey and Blanchard (1970), Bos (1976, 1989), Achour et al. (2003), and Achour and Amara (2021e), among others. These studies have consistently highlighted the constraints of rectangular weirs in achieving precise flow measurement under conditions where minimal discharge is present. However, to mitigate these limitations and enhance measurement accuracy, specific design requirements have been established for these devices (SIA, 1926). These engineering refinements aim to minimize flow disturbances by ensuring smooth resulting flow, optimize hydraulic performance, and ensure reliable discharge calculations across a broad range of operating conditions.

The advancement of weir technology has been propelled by recent theoretical and experimental research aimed at refining the governing relationships of the discharge coefficient (C_d). These investigations seek to improve the predictive accuracy of discharge calculations, ensuring alignment with empirical observations across diverse flow conditions. For those interested in a comprehensive understanding of weirs featuring notches of common geometries, the following references, among others, provide fundamental insights into the principles and recent advancements in weir technology (Achour and Amara, 2021a; 2021b; 2021c; 2021d; 2021e; Achour et al., 2022a; Achour et al., 2022b). These contemporary studies systematically update and validate the theoretical frameworks governing discharge coefficients, bridging the gap between theoretical predictions and experimental findings, thereby enhancing their reliability for practical hydraulic applications.

The selection of an appropriate weir design plays a critical role in determining the accuracy and reliability of flow measurement. Among the most effective designs, weirs without a crest height offer significant advantages, particularly due to their self-cleaning geometry, which prevents sediment buildup and ensures consistent flow depth readings. This characteristic makes them particularly valuable in applications where precision is of utmost importance. Conversely, rectangular weirs may still be suitable for scenarios where accommodating a broader range of flow rates is prioritized over achieving the highest level of measurement accuracy.

Recent advancements in flow measurement technology have been extensively documented in the literature, with particular emphasis on circular thin-walled weirs and sharp-edged width constrictions. Cutting-edge research has led to significant progress in the modeling and analysis of circular thin-walled weirs, addressing both free-flow conditions and partially submerged scenarios. A novel theoretical framework has been introduced to enhance the predictive accuracy of discharge behavior for these devices. Notable contributions in this field include the pioneering works of Brandes and Barlow (2012), Vatankhah and Bijankhan (2013), and Amara and Achour (2021), which provide fundamental insights into the hydraulic performance and operational efficiency of circular weirs.

Among the various flow measurement devices, sharp-edged width constrictions distinguish themselves through their simplicity, cost-effectiveness, and ease of implementation. Unlike traditional weirs, this device lacks a crest height, consisting of two vertical thin plates positioned transversely to the flow, forming a central opening of width b. This straightforward configuration is regarded as one of the simplest and most practical solutions for open-channel flow measurement.

In contrast to trapezoidal-shaped openings, as experimentally investigated by Farzad and Vatankhah (2023), the rectangular geometry of sharp-edged constrictions offers a more rigorous theoretical foundation. As highlighted by Achour and Amara (2021f; 2022g), this shape enables the analytical derivation of a discharge coefficient relationship that explicitly accounts for the influence of approach flow velocity. Their study demonstrated that the theoretical discharge coefficient (C_d) is exclusively governed by the contraction rate ($\beta = b/B$), where B represents the width of the rectangular approach channel. This dependency was initially predicted through dimensional analysis and later validated by both theoretical formulations and experimental observations.

Moreover, dimensional and experimental analyses confirmed that the relative upstream flow depth (h/B) has no effect on the discharge coefficient within the practical range of β. This key finding simplifies the practical application of the device across various hydraulic conditions. The agreement between theoretical predictions and experimental results was remarkable, with a maximum deviation of less than 2%. Further refinement, incorporating experimental corrections, reduced this deviation to just 1.36%, underscoring the high precision and reliability of the theoretical model (Achour and Amara, 2021f). In a subsequent study, Achour and Amara (2022g) conducted a comprehensive re-evaluation of the device from an experimental standpoint, significantly enhancing the quality and precision of the testing procedures compared to their previous investigation (Achour and Amara, 2021f). The study was designed to enhance both the qualitative and quantitative aspects of the experimental tests while simultaneously refining the theoretical framework governing the discharge coefficient of the device. This dual approach aimed to ensure greater accuracy, reliability, and consistency in the derived relationship, thereby strengthening its applicability in practical flow measurement scenarios. In this new experimental campaign, the theoretical and experimentally observed discharge coefficients were systematically compared. The results revealed an exceptionally low maximum deviation of less than 0.05%, reinforcing the accuracy and predictive capability of the theoretical model. These findings firmly establish the sharp-edged width constriction device as one of the most precise and high-performing flow measurement tools for rectangular open channels, offering unparalleled reliability in hydraulic engineering applications.

The study by Achour et al. (2025a) presents a comprehensive theoretical and experimental investigation into the application of the sharp-edged width constriction with rectangular opening for flow measurement in trapezoidal open channels. This research aimed to establish the effectiveness and reliability of this constriction as practical and precise flow measurement tool. To derive the governing discharge coefficient relationship, the study employed two well-established energy-based methodologies. Both theoretical approaches yielded identical results, confirming the robustness and consistency of the proposed

formulation. The analysis demonstrated that the discharge coefficient (C_d) is solely dependent on two dimensionless parameters: 1) The contraction rate $\beta = b_o/b$), where b_o is the opening width of the device, and b is the base width of the trapezoidal approach channel, 2) The non-dimensional parameter mh_1/b, where m represents the side slope of the trapezoidal channel, i.e., 1 vertical to m horizontal, and h_1/b is the relative upstream water depth.

The experimental program included an extensive dataset comprising 1,012 measurement points, covering a wide range of flow conditions. The observed experimental results were in excellent agreement with the theoretical predictions, with a maximum deviation of only 0.301%. This exceptionally low error margin attests to the high accuracy and reliability of the proposed theoretical discharge coefficient relationship.

The findings confirm that sharp-edged constrictions with rectangular openings provide a precise and reliable means of measuring flow rates in trapezoidal open channels. This research offers a practical, theoretically sound, and experimentally validated tool for flow measurement applications in irrigation systems, hydraulic engineering projects, and environmental monitoring. In addition, the robust theoretical framework minimizes the need for empirical calibrations, enhancing the practical applicability and efficiency of the method in real-world hydraulic systems.

In recent years, innovative flow measurement devices have been extensively investigated through both theoretical modeling and experimental validation to establish precise stage-discharge relationships. Among these advancements, broad-crested weirs - available in triangular and rectangular configurations, with or without crest heights - have emerged as versatile and reliable solutions for open-channel flow measurement.

Both thin-crested and broad-crested weirs continue to hold substantial practical significance in hydraulic engineering, playing a crucial role in various hydraulic structures due to their adaptability, accuracy, and ease of implementation. Their widespread use underscores their fundamental role in flow regulation and discharge quantification across diverse hydraulic applications.

To gain a comprehensive understanding of the latest advancements in the various uses of weirs and their technology, the literature offers an extensive selection of key references. Notable recent contributions include studies by Achour and Amara (2020, 2022a, 2022d, 2022e, 2023a), as well as Achour et al. (2022b, 2022c), which have significantly expanded the theoretical and experimental foundations of discharge measurement techniques. Additionally, Kulkarni and Hinge (2021, 2023) have introduced pioneering research focusing on compound broad-crested weirs and the integration of additive manufacturing to enhance the performance and precision of flow measurement devices.

Weirs with a longitudinal triangular profile, such as the Bazin and Crump weirs, are well-established devices for flow measurement in open channels. Despite their geometric similarities, these weirs differ in their upstream and downstream slope configurations, which influence their hydraulic performance and practical implementation. The Bazin weir, developed in 1898, features four different combinations of upstream and downstream slopes, providing a greater range of design flexibility (Bazin, 1898). In

contrast, Crump simplified the design to a standardized 1:2 upstream slope and 1:5 downstream slope, making it easier to construct and implement in the field (Henderson, 1966; Bos, 1976; Hager, 1986; Achour et al., 2003).

However, both Bazin and Crump weirs have limited applications, as they are primarily designed for rectangular open-channel flow measurement, restricting their adaptability to channels of varying geometries. Furthermore, Bazin's weir did not achieve widespread adoption due to a critical design limitation - it was calibrated for a large crest height (P = 50 cm), which proved impractical for industrial channels of its time (Afblb, 1970). This shortcoming has remained unaddressed in subsequent studies, further diminishing its practical relevance in modern hydraulic applications.

The latest advancements in the study of Crump weirs are thoroughly documented in the works of Zuikov (2017) and Achour and Amara (2022f), with a primary focus on refining the stage-discharge relationship, a fundamental aspect of flow measurement accuracy. Zuikov's research introduced a stage-discharge equation that, despite making a notable contribution to the field of flowmetry, exhibited a 5% deviation in flow rate calculations. However, it was later identified as incomplete due to a critical oversight. In response, Achour and Amara (2022f) conducted an in-depth investigation and pinpointed a significant omission in Zuikov's model - the relative upstream flow depth (h/B), where h represents the flow depth above the weir crest and B denotes the width of the rectangular approach channel. Their findings revealed that h/B plays a crucial role in influencing the discharge coefficient (C_d), with an average impact of 23.5%.

To rectify this limitation, Achour and Amara (2022f) developed a new stage-discharge relationship that explicitly incorporates the h/B parameter, ensuring a more precise and comprehensive formulation. This revised model demonstrated an exceptionally low maximum deviation of just 0.864% in the computation of both the discharge coefficient (C_d) and the flow rate (Q) under free overflow conditions. Consequently, the relationship proposed by Achour and Amara (2022f) is regarded as the most accurate and refined (C_d) formulation ever developed for Crump weirs, marking a significant breakthrough in hydraulic engineering and advancing flow measurement accuracy to an unprecedented level.

Achour and Amara (2023b) recently introduced the "2A Triangular Weir," a longitudinal-profile triangular weir named in recognition of its creators. This innovative weir has been extensively analyzed through design optimization, theoretical modeling, and experimental validation. The upstream and downstream slope values of the "2A Triangular Weir" are identical to those of the Crump weir, a deliberate design choice aimed at ensuring optimal flow adhesion to the weir's surfaces and enhancing hydraulic efficiency.

In contrast to the Crump and Bazin weirs, which are characterized by rectangular cross-sections, the "2A Triangular Weir" is entirely composed of triangular cross-sections - a shape widely recognized in flowmetry for its superior hydraulic performance. This fundamental distinction extends its applicability across all open-channel configurations, making it a universal flow measurement device. The triangular cross-section enables

more precise readings of upstream water depths, facilitating highly accurate discharge estimations.

In addition, the elimination of transitional discontinuities between the weir and channel walls ensures that the discharge coefficient (C_d) remains independent of the relative upstream depth, a notable limitation in Crump weirs. Classified as a semi-modular flow measurement device, the "2A Triangular Weir" exhibits a discharge that is influenced by both its geometric design and the upstream water depth above the crest. This unique hydraulic behavior has been thoroughly confirmed through Achour and Amara's extensive research, establishing the "2A Triangular Weir" as a highly effective and versatile tool for flow measurement in open channels.

Flumes, renowned hydraulic structures, have been extensively utilized for accurate flow measurement in open channels. These devices are specifically engineered to regulate, direct, and quantify water flow across a wide range of applications, including hydrological studies, irrigation networks, wastewater treatment facilities, and comprehensive water resource management systems. The fundamental purpose of a flume is to create a controlled hydraulic environment where the flow rate can be precisely monitored and analyzed.

Flumes are commonly designed with specific geometric configurations, such as parabolic, trapezoidal, or V-shaped cross-sections, each tailored to optimize hydraulic efficiency and flow control. When properly designed and implemented, they establish a stable and uniform flow regime, which is crucial for ensuring highly accurate discharge measurements.

The flow rate within a flume is typically determined by correlating the measured water depth at a designated location with empirical stage-discharge relationships. These pre-established formulas account for key factors such as flume geometry, upstream water depth, and prevailing hydraulic conditions. In addition to their primary function as flow measurement instruments, flumes are integral components of water regulation systems, ensuring that flow rates are maintained within specified limits while minimizing uncontrolled turbulence and hydraulic losses.

Despite their structural simplicity, flumes are engineered for durability and long-term performance. They are commonly constructed from robust materials such as concrete, steel, or masonry, ensuring resilience under varying hydraulic loads and prolonged exposure to fluctuating flow conditions. Their longevity and reliability make them essential tools in modern water management and hydraulic engineering applications.

Over time, several well-established flume designs have been developed and extensively studied to enhance flow measurement accuracy and hydraulic efficiency. Among the most recognized are, Parshall Flume (1936) – A widely used flume known for its precision in open-channel flow measurement, Venturi Flume – Developed in both its original and modified forms (Bos, 1976; 1979; Achour et al., 2003; Hager, 1986), this flume was specifically designed to improve accuracy in flow control and measurement, Trapezoidal Flume – Recognized for its effectiveness in regulating water flow (Open Channel Flow, 2024), New Trapezoidal Flume – Recently introduced through a comprehensive

theoretical and experimental study (Achour et al., 2024), this flume distinguishes itself through its simplified design, ease of implementation, and unmatched precision, Modified Montana Flume – A recently enhanced version (Achour et al., 2024) that provides superior hydraulic performance, H-Flume – A well-known flume that continues to undergo modifications for improved accuracy and operational control (Achour et al., 2025b).

A notable limitation of most conventional flumes is that they primarily feature rectangular cross-sections, which can lead to reduced measurement accuracy at low flow rates. To overcome this challenge, Achour and De Lapray (2023) developed a novel flume with a triangular cross-section, offering remarkable precision in measuring both high and low flow rates. This innovative design presents the additional advantage of being self-cleaning, facilitated by its flat-bottom configuration, which enables the efficient passage of sediments and small debris - a crucial factor in maintaining measurement accuracy.

For a detailed exploration of this newly developed flume, including its design methodology based on fundamental geometric principles, readers are encouraged to consult the previously referenced study. The study also provides a rigorous formulation of the governing equations, ensuring a robust theoretical framework for transition flow analysis and device optimization.

With particular emphasis on triangular open approach channels, which constitute the primary focus of this study, it is generally true that simple and inexpensive methods for directly measuring flow rates in such channels are not widely available. Unlike rectangular or trapezoidal channels, where weirs and flumes provide relatively simple and cost-effective solutions, triangular channels pose unique challenges due to their continuously varying width with depth, making it difficult to develop straightforward stage-discharge relationships. A common but relatively expensive method such as current meters, where velocity is measured at multiple points in the cross-section, and the total discharge is computed using the velocity-area method. Ultrasonic flow meters are often used – These advanced electronic devices use Doppler or transit-time principles to measure velocity and estimate discharge. While highly accurate, they are costly and require calibration. Electromagnetic flow meters are sometimes preferred – These meters measure voltage induced by the conductive properties of water moving through a magnetic field, providing an accurate but expensive flow measurement solution. Acoustic Doppler Velocimeters (ADV)–Used primarily for research applications, these instruments measure velocity profiles in open channels, including triangular ones, but they are costly and require expertise.

The End-Depth Method (EDM) is a widely used and practical technique for estimating flow rates in open channels, including those with triangular cross-sections (Rouse, 1949; Chow, 1959; Diskin, 1961; Rajaratnam and Muralidhar, 1964). This method capitalizes on the relationship between the measured end-depth (h_e) at the downstream extremity of the channel, also called the brink depth, and the critical depth (h_c), which serves as a fundamental parameter for determining the discharge Q using established critical flow equations. For a triangular channel with side slopes of 1:m, the critical depth (h_c) is commonly expressed as $h_c = kh_e$, where k is an empirical coefficient that depends on the

channel geometry and flow conditions. Several researchers have conducted experimental and theoretical studies to derive appropriate values of k for different triangular channel configurations where the flow is in a subcritical state. For such channel shape, the coefficient k typically varies within the range $1.14 \leq k \leq 1.20$ (Hager, 1983; Muhsin et al., 2021; Dey, 2002; Nabavi et al., 2024). However, a detailed examination of Ferro's (1999) study reveals that, for the triangular channel, the maximum value of k, attained at a Froude number $F_1 = 1$ (Control section), is $k = 1.1307$, thereby broadening the previously indicated range of k, which can be written as $1.1307 \leq k \leq 1.20$.

It is important to note that the aforementioned maximum value of k (1.1307) was derived exclusively for smooth triangular channels. In practical scenarios, particularly for man-made canals, the channel walls typically exhibit varying degrees of surface roughness, characterized by their absolute roughness. This factor significantly influences the hydraulic behavior of the flow and, consequently, the value of the k coefficient. As a result, k may deviate substantially from the theoretical value established for ideal smooth channels.

Numerous researchers have established varying values of the coefficient k, influenced by factors such as channel geometry, experimental conditions, and the underlying assumptions applied in their analyses. This variability in k inherently affects the accuracy of discharge (Q) calculations, making it a critical consideration when employing the End-Depth Method (EDM) for practical flow measurements. This issue is particularly pronounced in triangular channels, where the relatively high sensitivity of k introduces a potential source of computational error. Even minor fluctuations in k can result in significant deviations in the estimated flow rate, underscoring the need for precise determination and careful application of this coefficient in discharge assessments. Therefore, without standardized k values that account for channel roughness and other site-specific factors, the use of (EDM) for flow measurement in triangular channels should be approached with caution.

To illustrate the influence of inaccuracies in both the estimation of k and the measurement of h_e on the discharge Q computation, it is essential to consider the relative error $\Delta k/k$ inherent in estimating the coefficient k within the range of 1.14 to 1.20, even to 1,2988. This uncertainty directly propagates into the discharge calculation, leading to a relative error in Q expressed as $\Delta Q/Q = 2.5 \times \Delta k/k$. In addition, the overall discharge error is further compounded by the measurement uncertainty in the end-depth h_e, contributing an additional term of $2.5 \times \Delta h_e/h_e$, meaning that $\Delta Q/Q = 2.5 \times \Delta k/k + 2.5 \times \Delta h_e/h_e$.

Consequently, both the uncertainty in k and the precision of h_e measurements play a crucial role in determining the reliability of the computed discharge when using (EDM).

Consequently, while EDM provides a straightforward and cost-effective means of flow measurement, its accuracy is highly dependent on precise empirical calibration and field validation.

According to the specialized literature, Manning's equation is widely used in practice to determine the discharge Q conveyed by a triangular channel. This equation allows for the practical computation of Q if the flow depth h, side slope m, Manning's roughness

coefficient n, and bed slope S are known. However, in this approach, Manning's coefficient n is erroneously assumed to be a constant, solely dependent on the channel material, which is evidently an entirely incorrect assumption. It has been rigorously demonstrated that Manning's coefficient n is intrinsically linked to the relative roughness ε/R_h, where R_h is the hydraulic radius, as well as to the shear Reynolds number Re^*.

There is lack of standardized weirs or flumes – Unlike rectangular and trapezoidal channels - no well-established, low-cost weirs or flumes specifically designed for triangular channels exist.

Complex flow profiles–Triangular cross-sections result in non-uniform velocity distributions, making it difficult to use simple stage-discharge equations.

High Sensitivity to wetted area variations–Since the wetted area changes with depth in a non-linear manner, small errors in depth measurement can lead to large discharge calculation errors.

Developing a low-cost, simple device such as a modified weir or flume tailored for triangular channels could significantly improve flow measurement accessibility. A specially designed V-notch without crest height P, similar to a contracted triangular weir but adapted for a triangular open approach channel, could be an innovative and cost-effective solution. Moreover, the deliberate selection of this particular configuration is intended to eliminate the influence of the relative crest height ratio P/h on the discharge coefficient (C_d), where and h is the upstream water depth over the crest. This consideration is especially important in the context of thin-crested weirs, where existing analytical approaches - based on energy or momentum principles - are insufficient to accurately account for the effects of the relative crest height P/h on (C_d), which is the key dimensionless parameter that characterizes the degree of vertical contraction experienced by the flow as it approaches and passes over the thin-crested weir. In such cases, the influence of P/h on (C_d) can only be captured through empirical modeling, due to the complex interplay between flow contraction, streamline curvature, and nappe formation. By excluding this variable, the configuration ensures a more precise evaluation of other governing parameters affecting the discharge coefficient.

Positioning such a V-notch at the downstream end of the triangular channel, where the flow rate needs to be determined, represents the most practical and straightforward solution. This configuration offers ease of implementation while ensuring a reliable and efficient method for measuring discharge conveyed by such canals.

This study aims to explore and establish this solution through a comprehensive theoretical framework and rigorous experimental validation, ensuring both its accuracy and practical applicability. The primary objective of this study is to develop a rigorous theoretical formulation governing the discharge coefficient (C_d) of the V-notch. This formulation will serve as the foundation for accurately determining the desired flow rate (Q) passing through the V-notch, utilizing the fundamental discharge equation in its conventional form.

To validate the theoretical formulation of the discharge coefficient (C_d) or refine it, if necessary, a comprehensive experimental program is planned. This program will involve testing V-notches with varying geometric configurations under realistic flow conditions, ensuring that the full range of possible hydraulic scenarios is thoroughly examined.

The method proposed by the authors for measuring flow in triangular channels is particularly suited for situations where alternative methods, such as EDM and EDR, are not applicable. While free fall at the terminal section is an idealized condition for methods like EDM and EDR, it is not always present in real-world triangular channels. Factors such as downstream submergence, the presence of a hydraulic jump, the presence of a hydraulic structure such as a sluice gate that limits the downstream flow, and so on, can all prevent the establishment of free-falling flow at the terminal section.

This can also happen for irrigation canals, often with triangular cross-sections, which, for reasons of topographic constraints, sometimes have horizontal segments, sometimes segments with a positive slope, or a terminal segment with a negative slope. In this case, methods such as EDM and EDR cannot be applied.

Consequently, in numerous practical applications, alternative flow measurement methods may be necessary, such as the approach explored in this study for measuring flow in triangular open channels.

MATERIAL AND METHODS

Description of the hydraulic installation and resulting flow profile

Fig. 1 presents a perspective view of the hydraulic installation under investigation comprises a triangular open-channel that functions as the approach channel. At its downstream end, this channel transitions into a contracted V-notch formed by two thin triangular plates, labeled ABCA and A'B'CA', as illustrated in Fig. 2. As depicted in this figure, the plates are securely riveted into the thickness of the end section of the approach channel. During the experimental study, a joint was meticulously placed between the V-notch plates and the terminal section of the triangular open approach channel to ensure a perfect seal.

It is important to note, however, that the triangular plates shown in Fig. 2 can also be positioned at any cross-section of the triangular open approach channel. This configuration is particularly advantageous when the terminal section of the triangular approach open channel is either obstructed, inaccessible, or unreachable, such as when a hydraulic structure is present. In this arrangement, a secure seal around the plates can be effectively ensured by applying a silicone joint around the downstream side perimeter of the chosen cross-section.

The side slope of the triangular open approach channel is denoted as $m_1 = \cot(\alpha)$, corresponding to an inclination of 1 vertical to m_1 horizontal (Fig. 1). In contrast, the side slope of the V-notch is represented by $m_2 = \cot(\theta)$, signifying an inclination of 1 vertical to m_2 horizontal (Fig. 1). As depicted in Fig. 1, the opening width b at the crest of the V-

notch is directly related to the side slope m_2, and its relationship can be expressed as follows:

$$m_2 = \frac{b}{2h_o} \tag{1a}$$

where h_o is the depth of the triangular open approach channel (Fig. 1).

Similarly, it may be expressed the following:

$$m_1 = \frac{T}{2h_o} \tag{1b}$$

where T is the top width of the triangular open approach channel (Fig. 1).

Eq. (1a) proves to be highly valuable, as it enables the precise determination of the side slope m_2. Given that the linear dimensions b and h_o can be measured with exceptional accuracy using standard instrumentation, Eq. (1) offers a remarkably reliable method for calculating m_2. Consequently, there is no need to perform a direct measurement of the angle θ on-site to determine m_2 through the previous trigonometric $m_2(\theta)$ relation. Such angular measurements are inherently susceptible to observational errors and may compromise precision.

It is important to emphasize that, in the course of the experimental investigation, the depth h_o of the triangular open approach channel will not be measured directly. Instead, its value will be determined indirectly through the application of Eq. (1b). This methodological choice is justified by the specific geometry adopted in the study, where the apex angle of the triangular open approach channel is set at 90°. Under these conditions, the side slope m_1 equals 1, which simplifies the geometric relationship governing the channel's cross-section. Accordingly, Eq. (1b) reduces to $h_o = T/2$. By measuring T with precision, the corresponding depth h_o can be accurately deduced. This indirect measurement approach is preferred because determining T is typically more precise and less prone to experimental error than attempting to directly measure the channel depth h_o.

As illustrated in Fig. 1, the base of the triangular open approach channel is elevated 35 cm above the platform by means of a robust support structure. This elevation is purposefully designed to facilitate optimal aeration of the free-flowing water nappe as it emerges from the V-notch, as depicted in Fig. 3. By ensuring sufficient clearance beneath the flow, this configuration minimizes the potential for surface tension effects and preserves the free-fall characteristics of the jet, thereby maintaining the integrity of the flow profile and ensuring accurate discharge measurement.

Moreover, unlike conventional flumes, the device in question offers the distinct advantage of being easily fabricated and assembled directly on-site. This flexibility allows for seamless customization to match the specific dimensions and geometric characteristics of the existing approach channel, eliminating the need for prefabricated structures and ensuring an optimal fit within diverse hydraulic installations.

The choice of material for constructing the V-notch is primarily determined by the characteristics of the conveyed water and the nature of any suspended sediments it may carry. For example, stainless steel is widely preferred in cases where the flow contains chemical agents or abrasive solid particles, due to its superior resistance to corrosion and wear.

Owing to the design configuration of the system - particularly the V-notch without a crest height - the longitudinal axis of the device remains horizontal. This horizontal alignment ensures that any debris or solid materials entrained by the flow are unable to accumulate at the entrance of the notch. Instead, these materials are effectively transported downstream by the current, conferring upon the device a self-cleaning capability that minimizes maintenance requirements.

As illustrated in Fig. 3, the resulting longitudinal flow profile clearly demonstrates a subcritical flow regime prevailing in the approach channel upstream of the V-notch. This flow condition was consistently observed across all the V-notch geometries tested in this study. Conversely, downstream of the V-notch, the flow transitions to a supercritical regime, characterized by high velocities and a concentrated water jet. The transition between subcritical and supercritical flow regimes signifies the presence of a control section at the V-notch, where the flow passes through critical depth conditions. The presence of a control section, characterized by critical flow conditions, constitutes a *sine qua non* condition for the accurate and reliable operation of the V-notch as a flow measurement device.

It is therefore both logical and hydraulically justified to designate section 2-2 in Fig. 3, located at the V-notch, as the critical control section. This is the point at which the flow depth corresponds to critical flow conditions, and its associated hydraulic parameters are denoted with the subscript "*c*". However, it is important to note that, to date, no analytical or experimental method has been able to precisely determine the exact location of this control section with absolute accuracy.

Upstream of the V-notch, the flow depth - designated as h_1 - can be considered constant starting from section 1-1. This stability is attributed to the presence of the contraction device, which effectively dampens upstream flow disturbances and reduces the influence of approach flow velocity. This hydraulic behavior is particularly advantageous, as it facilitates precise and reliable measurement of the upstream depth h_1, a critical parameter in accurately determining the discharge Q conveyed by the system (Fig. 3).

Despite the exceedingly short length of the V-notch along the flow direction, which corresponds to a low thickness, a control section - commonly known as the critical section - inevitably forms. The existence of this control section is a fundamental prerequisite for the accurate functioning of the device as a flow measurement instrument. Its role is pivotal in establishing the validity of the theoretical stage-discharge relationship that governs the device's performance.

When employing the device configuration illustrated in Fig. 1, the measurement of the upstream flow depth, denoted h_1, is systematically taken at a fixed location upstream of the V-notch. This designated measurement point remains consistent, irrespective of the

physical dimensions or geometric variations of the device. This feature contrasts sharply with many conventional flumes, such as the Montana Flume, where the location for measuring h_1 must be carefully determined according to the specific dimensions of the flume (Open Channel Flow, 2024). In such cases, strict adherence to the prescribed measurement location is imperative; any deviation may result in substantial errors in the computed flow rate when applying the stage-discharge relationship associated with that device.

By maintaining a fixed and well-defined measurement section for h_1 in the proposed V-notch configuration, the risk of user error is minimized, enhancing both the reliability and simplicity of flow rate determination.

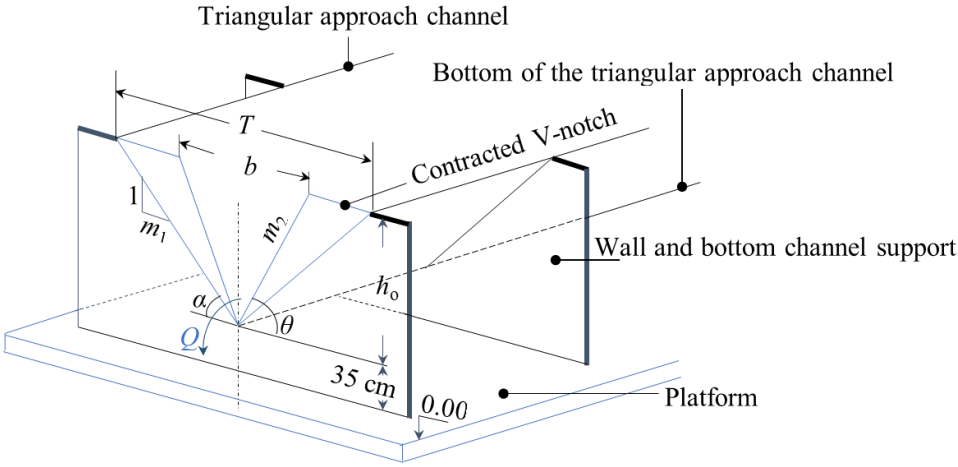

Figure 1: Geometric definition and configuration of the crestless V-Notch installed in a triangular open approach channel for flow measurement

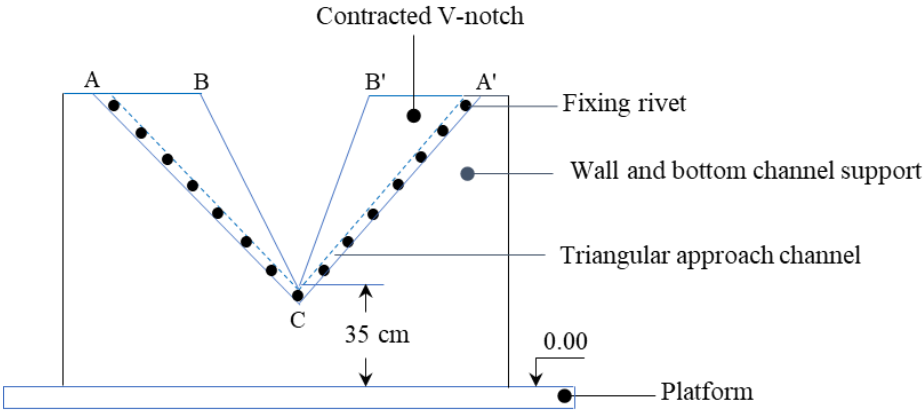

Figure 2: Downstream view of the V-notch fixed by rivets at the terminal section of the triangular open approach channel

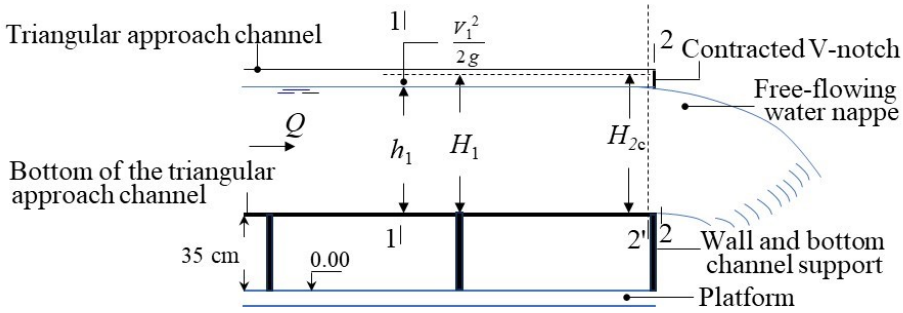

Figure 3: Longitudinal flow profile resulting from the authors' proposed hydraulic measuring device

Section reduction ratio

The section reduction ratio is conventionally defined as the ratio of the downstream flow cross-sectional area to the upstream flow cross-sectional area. In the context of the present study, let us denote the wetted flow area at section 1-1 of the triangular open approach channel as A_1, and the wetted flow area at section 2'-2', located immediately upstream of the V-notch, as A_2 (Fig. 3). Given that both sections exhibit triangular cross-sectional geometries, their respective areas can be expressed by the following well-known mathematical relationships:

$$A_1 = m_1 h_1^2 \tag{2}$$

$$A_2 = m_2 h_1^2 \tag{3}$$

Their ratio is as follows:

$$\frac{A_2}{A_1} = \frac{m_2 h_1^2}{m_1 h_1^2} = \frac{m_2}{m_1} \tag{4}$$

Since the V-notch under consideration is specifically designed such that $m_2 < m_1$, the wetted area A_2 is reduced compared to the wetted area A_1, indicating a geometric contraction of the flow cross-section, which directly affects flow behavior, velocity distribution, and hence the discharge coefficient. In classical flow measurement devices, e.g., weirs, flumes, the contraction ratio is often defined as the ratio of the reduced section width to the original width. Herein, since we are dealing with triangular cross-sections, the side slopes m_1 and m_2 play the role of width descriptors. Thus, the ratio m_2/m_1 effectively represents the reduction in flow cross-section, and can indeed be considered as the section reduction ratio in this specific case.

In order to quantitatively characterize the contraction phenomenon within the channel, the dimensionless parameter ζ, referred to as the section reduction ratio, is introduced. This parameter provides a measure of the relative decrease in cross-sectional area due to the geometric configuration of the approach channel. Mathematically, ζ is defined by Eq. (4). Furthermore, by incorporating the relationships established in Eqs. (1a) and (1b), the expression for ζ can be reformulated as follows:

$$\zeta = \frac{m_2}{m_1} = \frac{b}{T} \tag{5}$$

The dimensionless parameter ζ provides a direct measure of the extent to which the flow cross-section is reduced at the V-notch relative to the approach channel. Thus, ζ is less than 1, varying within the following range $0 < \zeta < 1$. The limiting cases where $\zeta \to 0$ and $\zeta \to 1$ are excluded from any practical analysis, as such conditions are not physically attainable in real-world applications. These extremes represent theoretical boundaries that do not correspond to feasible hydraulic configurations.

A lower value of ζ indicates a more pronounced contraction, while a value approaching 1 signifies minimal or no flow constriction in this extreme case. In addition, acting in the capacity of a section reduction ratio, ζ governs the flow transition through the device.

As will be demonstrated in the relevant section of this study, the dimensionless parameter ζ serves as a fundamental determinant in characterizing the discharge coefficient of the contracted V-notch under investigation, directly influencing the flow behavior and hydraulic performance of the system.

To ensure the existence of a critical flow regime in the V-notch placed at the downstream end of a triangular channel, the side slope m_2 of the V-notch must be carefully selected.

For the flow to be critical at the notch, the critical depth (h_c) must be physically possible and must satisfy energy and momentum conditions across the contraction. If m_2 is too large, the notch becomes too wide, preventing the establishment of a control section at the V-notch.

The maximum allowable side slope m_2 is constrained by the section reduction ratio ζ, ensuring: sufficient flow contraction, the need for a control section where critical depth can exist, thus inducing a proper functioning of the V-notch as a flow measuring device, and practical hydraulic constraints preventing excessive flow expansion.

From authors' experimental studies and theoretical analysis, a reasonable upper bound for ζ ensuring critical flow at the notch is $\zeta \leq ½$, meaning that $m_2 \leq m_1/2$ according to Eq. (5). Thus, the V-notch side slope m_2 should not exceed half the triangular open approach channel side slope m_1. This ensures that the notch remains sufficiently narrow to induce critical flow while still allowing an efficient discharge process. Exceeding this threshold may prevent the formation of a critical flow regime at the notch, leading to an uncontrolled flow that cannot be effectively used for flow measurement.

Conversely, the section reduction ratio ζ must not be excessively small to prevent the onset of surface tension effects within the V-notch under consideration. The presence of surface tension could substantially compromise the accuracy and reliability of the proposed theoretical framework, as this study does not account for surface tension influences in its analytical formulation. Ensuring an adequately high ζ value is therefore essential to maintaining the validity of the theoretical approach and minimizing deviations from expected flow behavior.

Surface tension becomes significant when the flow depth at the notch is very small, leading to potential errors in: 1) Flow contraction behavior affecting the discharge coefficient (C_d), 2) Stage-discharge relationship, introducing non-negligible capillary forces, 3) Experimental measurements, where flow instabilities at low depths make depth readings uncertain. According to in-depth investigations of the authors, to ensure that surface tension does not significantly impact flow measurement in the V-notch, the minimum recommended value of the section reduction ratio ζ should be at least 0.3 to 0.4. If $\zeta < 0.3$, the flow depth at the notch becomes too small, and surface tension effects may introduce errors. If $\zeta > 0.4$, the flow remains sufficiently deep to ensure the dominance of inertial and gravitational forces, making surface tension negligible.

Therefore, in light of the aforementioned considerations and to ensure the reliability of both the theoretical and experimental approaches, the authors recommend selecting the section reduction ratio ζ within the safety optimal range of $0.35 \leq \zeta \leq 0.50$. This range strikes a balance between maintaining critical flow conditions within the V-notch and mitigating undesirable surface tension effects, thereby preserving the accuracy and applicability of the proposed methodology.

Furthermore, in practical applications, selecting values of ζ within the range of 0.35 to 0.50 ensures several critical outcomes: it facilitates a controlled contraction necessary for precise discharge measurement, promotes flow stability by maintaining a well-defined control section, and minimizes the risk of extreme flow sensitivity, which could otherwise result in unpredictable fluctuations in measurements.

On the other side, the previously specified recommended range for the section reduction ratio ζ directly translates, through the application of Eq. (5), into a corresponding recommended range for the ratio b/T, expressed as $0.35 \leq b/T \leq 0.50$. This relationship implies that the optimal values for the top width b of the V-notch should fall within the interval $0.35T \leq b \leq 0.50T$. In practical terms, the known quantity during the design and implementation phases is typically the top width T of the triangular open approach channel. This known dimension facilitates the precise determination of the V-notch opening b limit values, ensuring compliance with the recommended geometrical criteria. Adhering to these guidelines is essential to guarantee the proper hydraulic performance and accuracy of the V-notch weir under operational conditions.

Dimensional analysis and the crestless contracted V-notch discharge coefficient dependency

In this section, dimensional analysis is utilized to establish the general formulation of the governing physical equation for the discharge coefficient of the V-notch under investigation. This methodology ensures that the derived equation not only provides an accurate representation of the underlying hydraulic behavior but also maintains dimensional consistency, meaning that all terms align with fundamental unit principles. In addition, it facilitates the identification of key influencing factors while expressing the relationship in a reduced and simplified dimensionless form, enhancing its applicability and interpretability.

As an initial step, dimensional analysis necessitates the identification of all variables that significantly influence the discharge coefficient (C_d) of the considered V-notch. These variables are then systematically transformed into a set of dimensionless parameters, effectively reducing the complexity of the governing equation while preserving the essential physical relationships governing the flow through the V-notch.

The identification of influential parameters in dimensional analysis is typically guided by engineering expertise, physical intuition, and established principles of fluid mechanics. This selection process ensures that only the most relevant variables governing the phenomenon are considered, thereby simplifying the analytical framework while maintaining its accuracy.

In the present study, the discharge (Q) through the V-notch is primarily influenced by the following key parameters, which encapsulate the geometric, kinematic, and dynamic characteristics of the flow:

- Q Discharge (m^3/s) – the primary quantity of interest.
- h_1 Upstream flow depth (m) – determines the hydraulic head.
- m_1 Side slope of the triangular open approach channel, i.e., 1 vertical to m_1 horizontal.
- m_2 Side slope of the V-notch, i.e., 1 vertical to m_2 horizontal, – which affects flow contraction.
- g Acceleration due to gravity (m/s^2) – governs free-surface flow behavior.
- ρ Density of the fluid (kg/m^3) – influences flow properties.
- μ Dynamic viscosity of the fluid (Pa·s) – accounts for fluid resistance.
- σ Surface tension (N/m) – relevant for small-scale flows.

The interdependence among these variables can be mathematically formulated through the following functional relationship:

$$f\left(Q,\rho,g,h_1,\mu,\sigma,m_1,m_2\right)=0 \tag{6}$$

After identifying the key variables influencing the discharge process, the next critical step in dimensional analysis involves applying the Vaschy-Buckingham π theorem (Langhaar, 1962). This theorem serves as a fundamental framework for transforming complex physical relationships into a more concise, dimensionless form. By systematically implementing this theorem in conjunction with Eq. (6), a functional relationship can be established that expresses the discharge (Q) exclusively in terms of dimensionless parameters. This approach not only reduces the number of independent variables but also facilitates the derivation of a universally applicable equation, ensuring broad relevance across different flow conditions. Moreover, it enables the identification of the principal dimensionless groups governing the flow behavior, thereby enhancing the theoretical and practical understanding of discharge dynamics.

In hydraulic engineering, the stage-discharge relationship for a triangular weir is extensively documented in the literature (Bos, 1989; Hager, 1986; Achour and Amara, 2021a). This well-established formulation serves as a fundamental reference for evaluating flow characteristics over V-notches or triangular outlet sections. It is unequivocally demonstrated that the discharge (Q) passing through a V-notch is directly proportional to the side slope m of the notch, $h_1^{5/2}$, and $\sqrt{g}$.

By leveraging this theoretical framework, engineers can accurately predict discharge rates, optimize hydraulic structures, and enhance flow measurement techniques in various applications.

By implementing the Vaschy-Buckingham π theorem, the discharge Q appearing in the functional relationship (6), can ultimately be expressed as a function of a carefully derived set of dimensionless parameters. This transformation not only simplifies the governing equation but also ensures its applicability across various flow conditions, providing a more comprehensive understanding of the underlying physical phenomena. Considering the above considerations, the resulting (Q) functional relationship is formulated as follows:

$$Q = \sqrt{g}\, m_2\, h_1^{5/2} \gamma\left(\frac{\rho\sqrt{g}\, h_1^{3/2}}{\mu}, \frac{\rho g h_1^2}{\sigma}, \frac{m_2}{m_1} \right) \tag{7}$$

By integrating the well-established stage-discharge equation for triangular weirs with Eq. (7) from the present study, a comprehensive and refined functional relationship governing the discharge coefficient (C_d) is systematically derived. This formulation ensures a more precise characterization of flow behavior, accounting for the geometric and hydraulic parameters influencing discharge through the V-notch. Consequently, the discharge coefficient (C_d) is explicitly defined, capturing the intricate relationship between flow characteristics, geometric constraints, and hydraulic parameters. This formulation provides a fundamental basis for accurately predicting discharge behavior through the V-notch under various flow conditions. Thus, based on the formulation presented in the relationship (7), the discharge coefficient (C_d) is functionally identified as follows:

$$C_d = \gamma\left(\frac{\rho\sqrt{g}\,h_1^{3/2}}{\mu}, \frac{\rho g h_1^2}{\sigma}, \frac{m_2}{m_1}\right) \tag{8}$$

This functional relationship allows for a generalized and scalable approach to predicting the discharge coefficient (C_d), a direct connection between theoretical models and empirical observations, ensuring accuracy in flow measurement applications, and improved controllability and reliability of the V-notch under consideration, particularly in low and moderate flow conditions.

In the examination of flow dynamics within the considered V-notch, two fundamental dimensionless numbers inherently arise from Eq. (8): the Reynolds number (Re) - represented by the first term in brackets—quantifies the ratio of inertial forces to viscous forces, while the Weber number (We) - denoted by the second term in brackets - captures the ratio of inertial forces to surface tension forces. These dimensionless parameters offer critical insight into the prevailing physical mechanisms governing discharge behavior, facilitating a deeper understanding of flow characteristics and ensuring precise flow measurement and analysis.

The influence of the Reynolds number (Re) is deemed negligible due to the predominance of turbulent flow conditions within the V-notch under consideration. In such a regime, inertial forces overwhelmingly dominate viscous forces, resulting in minimal impact of viscosity on the discharge coefficient. Similarly, the effect of the Weber number (We) is considered insignificant, as surface tension becomes a critical factor only at extremely low flow rates, where the upstream depth is shallow and small opening angles in the notch triangular cross-section could intensify surface tension effects. However, these conditions are absent in the present experimental setup. Given that the study focuses on moderate to high flow rates, where neither viscosity nor surface tension exerts a significant influence, these factors can be reasonably disregarded without compromising the accuracy of the analysis.

Since the Reynolds number (Re) and the Weber number (We) have a negligible impact on flow behavior under the given conditions, the (C_d) governing functional relationship (8) can be refined by excluding these terms. This simplification yields a more concise and practical formulation for discharge computations, which is expressed as follows:

$$C_d = \varphi\left(\frac{m_2}{m_1}\right) = \varphi(\zeta) \tag{9}$$

Eq. (9) unequivocally establishes that the discharge coefficient (C_d) of the considered V-notch is exclusively governed by the dimensionless parameter ζ. This finding signifies that the secondary influences, including viscosity and surface tension, are negligible in this context, leaving ζ as the dominant controlling factor. The functional dependence φ, which characterizes the relationship between (C_d) and ζ, will be systematically derived in the subsequent section through a rigorous theoretical framework based on well-established hydraulic principles.

THEORETICAL ANALYSIS AND DERIVATION OF THE DISCHARGE COEFFICIENT RELATIONSHIP

The transition from a subcritical to a supercritical flow regime induces the formation of a control section immediately downstream of the V-notch. This control section plays a pivotal role in ensuring the accuracy and reliability of flow measurement, as it establishes critical flow conditions essential for the proper functioning of the device.

From a theoretical standpoint, the discharge (Q) can be expressed as a single-valued function of the upstream flow depth h_1. This mathematical relationship signifies that: 1) For each specific value of upstream depth h_1 within the operational range of the device, there exists one unique corresponding discharge (Q), 2) The flow rate can be accurately determined by recording a single measurement of h_1, typically at a predefined location - commonly the entrance cross-section immediately upstream of the contraction device, 3) This fundamental principle underpins the stage-discharge relationship, which forms the basis for flow measurement using hydraulic structures.

The stage-discharge relationship establishes a direct and reliable connection between the measured upstream water depth and the corresponding discharge, enabling precise and practical application in field and laboratory conditions.

The objective of this section is to theoretically derive the stage-discharge relationship for the V-notch under consideration by first establishing the governing equation for the discharge coefficient (C_d).

To achieve this goal, the authors propose two distinct theoretical approaches. The first method is based on the energy equation in dimensionless form. It utilizes the energy conservation principle, rewritten in dimensionless terms, to express the relationship governing (C_d). The second method relies on the properties of a kinetic factor, which is closely linked to the approach flow velocity, providing an alternative means of deriving (C_d). Interestingly, both methods yield identical results, reinforcing the theoretical validity of the derived discharge coefficient relationship.

As will be demonstrated, by employing these two theoretical approaches, the discharge coefficient (C_d) for the V-notch under consideration can be rigorously established, leading to the derivation of the stage-discharge relationship.

Theoretical framework based on the dimensionless energy equation

To establish a reliable stage-discharge relationship for the proposed V-notch device in triangular open approach channels, a rigorous theoretical formulation of the discharge coefficient (C_d) is essential. This section presents a framework grounded in the conservation of energy principle, reformulated in dimensionless terms to account for the influence of geometric and hydraulic parameters. By leveraging the energy balance between the upstream section and the control section at the V-notch, the analysis isolates the key governing variables and provides a pathway for deriving an explicit relationship for (C_d). This approach not only enhances the theoretical understanding of flow

contraction in triangular geometries but also enables a more accurate and practical application of the device in real-world flow measurement scenarios.

The critical depth in the triangular cross-section 1-1 (Fig. 3) is written as:

$$h_{1c} = \left(\frac{2Q^2}{g m_1^2} \right)^{1/5} \tag{10}$$

Let us remember that the subscript « *c* » denotes the critical conditions.

On the other hand, the critical flow depth in the V-notch weir is expressed by the well-known formulation as follows:

$$h_{2c} = \left(\frac{2Q^2}{g m_2^2} \right)^{1/5} \tag{11}$$

Given the extremely short distance separating sections 1-1 and 2-2, as illustrated in Fig. 3, it is reasonable and justified to assume that head losses due to friction or turbulence between these sections are negligible. Consequently, equating the total energy heads at sections 1-1 and 2-2 yields the following relationship:

$$H_1 = H_2 = H_{2,c} = \frac{5}{4} h_{2c} \tag{12}$$

By incorporating Eq. (2), the expression for the total energy head at the triangular cross-section 1-1 (Fig. 3) can be formulated as follows:

$$H_1 = h_1 + \frac{Q^2}{2g m_1^2 h_1^4} \tag{13}$$

By simultaneously considering the formulations presented in Eqs. (12) and (13), the following expression can be derived:

$$h_1 + \frac{Q^2}{2g m_1^2 h_1^4} = \frac{5}{4} h_{2,c} \tag{14}$$

Let us define the dimensionless parameter h_1^* as the ratio of the upstream flow depth h_1 to the critical depth $h_{2,c}$ in section 2-2 (Fig. 3), which occurs at the control section within the V-notch. This parameter effectively characterizes the hydraulic state of the upstream flow in relation to the critical flow conditions imposed by the geometry of the V-notch. It is expressed as follows:

$$h_1^* = \frac{h_1}{h_{2,c}} \tag{15}$$

By normalizing each term of Eq. (14) with respect to the critical depth $h_{2,c}$, and incorporating the definition provided in Eq. (15), the following dimensionless expression is obtained:

$$h_1^* + \frac{Q^2}{2g m_1^2 h_1^4 h_{2,c}} - \frac{5}{4} = 0 \tag{16}$$

Eliminating Q^2 from Eqs. (11) and (16), the resulting expression can be derived as follows:

$$h_1^* + \frac{\frac{1}{2} g m_2^2 h_{2,c}^5}{2g m_1^2 h_1^4 h_{2,c}} - \frac{5}{4} = 0 \tag{17}$$

By substituting Eqs. (5) and (15) into Eq. (17), and performing the necessary algebraic simplifications, the following expression is obtained:

$$h_1^* + \frac{\zeta^2}{4 h_1^{*4}} - \frac{5}{4} = 0 \tag{18}$$

Eq. (18) can be reformulated into the following final expression, representing the definitive relationship derived from the preceding theoretical development:

$$h_1^{*5} - \frac{5}{4} h_1^{*4} + \frac{1}{4} \zeta^2 = 0 \tag{19}$$

It is important to emphasize that the upstream flow depth, h_1, is always greater than the critical depth $h_{2,c}$, which occurs at the control section within the V-notch. Consequently, the dimensionless parameter h_1^* defined by Eq. (15) as the ratio $h_1/h_{2,c}$, must inherently satisfy the condition $h_1^* > 1$. This inequality reflects the fundamental hydraulic relationship between the upstream subcritical flow regime and the critical conditions imposed by the V-notch geometry. In addition, the rigorous adherence to $h_1^* > 1$ is not merely a mathematical condition - it reflects the physical reality of controlled flow through the device, underpinning the reliability and accuracy of the proposed measurement system.

It is important to recall that, as demonstrated in an earlier section of this study, the section reduction ratio ζ is strictly less than unity and whose optimal values are recommended to be selected within the range $0.35 \leq \zeta \leq 0.50$.

In practical applications, the side slopes m_1 and m_2, which define the section reduction ratio ζ, are generally known or predetermined based on the design specifications. Under these conditions, Eq. (19) becomes a fundamental tool for determining the relative upstream flow depth h_1^*. However, it is important to note that this equation is implicit with respect to h_1^*. As a result, suitable methods must be employed to obtain accurate values of h_1^*. Several approaches can be considered for this purpose, namely: 1) Graphical Interpretation: By plotting the functional relationship represented by Eq. (19), users can

extract corresponding values of h_1^* for different values of the section reduction ratio ζ. This method offers a visual and intuitive means of approximation but may lack precision if not carefully executed; 2) Trial-and-Error Method: This iterative technique involves making successive substitutions of h_1^* into the equation until a satisfactory level of convergence is achieved. While conceptually simple, this method can be time-consuming without the aid of computational tool; 3) Numerical Computation: The most efficient and precise approach involves using numerical methods or dedicated computational algorithms, such as the Newton-Raphson method or other root-finding techniques. These methods allow for the accurate and rapid determination of h_1^*, particularly valuable in engineering practice where precision is critical.

Each of these methods, commonly used, provides a pathway to resolving Eq. (19), enabling the accurate prediction of h_1^*, which, as will be demonstrated, plays a crucial role in defining the discharge coefficient (C_d) of the V-notch under consideration.

However, the authors will present an accurate and practical approximate relationship to Eq. (19), in this case Eq. (20b), derived through a rigorous analysis of the functional behavior of the curve $h_1^*(\zeta)$. This approximation captures the essential characteristics and trends of the dimensionless upstream depth h_1^*as a function of the section reduction ratio ζ, offering a simplified yet highly reliable alternative for engineering applications where direct use of the exact equation may be complex or impractical.

For readers with a keen interest in the mathematical rigor underpinning the theoretical development, it is worth noting that an analytical solution to the implicit Eq. (19) can be obtained through the application of the perturbation method. This approach yields an explicit expression for the dimensionless upstream depth $h_1^*(\zeta)$ in the form of an infinite series expansion. To render the solution practically usable, the series must be truncated to an appropriate term such that the resulting approximation remains within an acceptable error margin. For the expansion series to the fourth-order in the perturbation solution, the maximum deviation introduced in the computation of $h_1^*(\zeta)$ is approximately 0.00080713% - a value nearly 3.5 times greater than the error associated with the simpler approximate Eq. (20b). Moreover, the analytical expression derived via the perturbation method could be perceived as relatively complex, algebraically cumbersome, and unwieldy, which may limit its practical utility despite its theoretical elegance.

In the appendix, the authors provide a detailed derivation of Eq. (20a), presented below, using the perturbation method. The analytical solution for $h_1^*(\zeta)$, obtained by truncating the series expansion to the fourth-order, is expressed as follows:

$$h_1^* = \frac{5}{4} - \left(\frac{8}{25}\right)^2 \zeta^2 - \frac{1}{5}\left(\frac{16}{25}\right)^4 \zeta^4 - \frac{13}{50}\left(\frac{32}{50}\right)^6 \zeta^6 - \frac{51}{125}\left(\frac{32}{50}\right)^8 \zeta^8 \tag{20a}$$

For values of h_1^* that possess physical relevance, specifically when $h_1^* > 1$, and in accordance with the precise formulation given by Eq. (19), the variation of h_1^* as a function of the section reduction ratio ζ is illustrated in Fig. 4. Fig. 4 reveals in particular: 1) h_1^* decreases as ζ increases, signifying that a greater section reduction ratio ζ results in

a shallower relative upstream depth h_1; and 2) The relationship adheres to the following specific boundary conditions: (ζ; h_1^*) = (0; 0.125) and (ζ; h_1^*) = (1; 1).

As noted in the paragraph dedicated to the section reduction ratio ζ, the extreme cases where $\zeta \to 0$ and $\zeta \to 1$ are excluded from practical analysis, as these conditions are not physically realizable in real-world applications using the V-notch for triangular open approach channels flow measurement. These extreme values represent theoretical limits that do not correspond to practical hydraulic configurations.

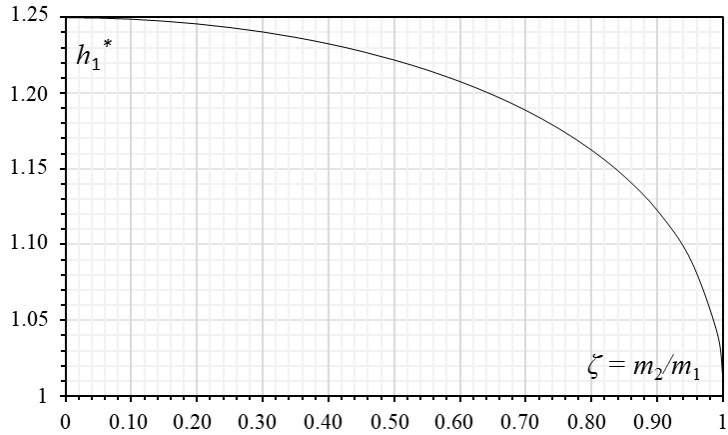

Figure 4: Variation of $h_1^*(\zeta)$ based on the precise formulation in Eq. (19)

A thorough examination of the variation of $h_1^*(\zeta)$, as illustrated in Fig. 4, demonstrates that the curve precisely coincides with a quarter of an ellipse. This geometric observation proves to be insightful, as it enables: 1) a more precise approximation of the implicit function defined by Eq. (19), and 2) the development of an explicit approximate formula to replace the implicit expression, thereby streamlining computational processes.

Consequently, by utilizing the mathematical properties inherent to an ellipse, the authors propose the following explicit relationship for $h_1^*(\zeta)$, strictly applicable within the recommended range of ζ, i.e., $0.35 \leq \zeta \leq 0.50$:

$$h_1^* = 0.291\left(1-\zeta^2\right)^{0.3521} + 0.959 \tag{20b}$$

Eq. (20b) exhibits exceptional accuracy, yielding a maximum deviation of merely 0.0002323% in the computation of the dimensionless upstream flow depth h_1^*, when compared to the exact implicit Eq. (19). Moreover, Eq. (20b) is highly recommended for the majority of engineering applications, owing to its mathematical simplicity coupled with its exceptional accuracy across the practical range of operating conditions $0.35 \leq \zeta \leq 0.50$.

To derive the stage-discharge relationship for the V-notch under consideration, a crucial step entails removing the critical depth $h_{2,c}$ from Eqs. (11) and (15). This mathematical manipulation results in a generalized stage-discharge equation, which establishes a direct

relationship between the discharge (Q) and the upstream depth (h_1). The resulting formula is as follows:

$$Q = \frac{1}{2}\sqrt{2g}\, m_2\, h_1^{*\,-5/2} h_1^{5/2} \tag{21}$$

The resulting Eq. (21) adheres to the conventional stage-discharge formulation, where the flow rate (Q) is a well-defined as a single-valued function of the upstream depth (h_1). This guarantees that each measured value of the upstream depth corresponds to a unique discharge value, thereby simplifying and ensuring the accuracy and reliability of flow measurements. Moreover, this theoretically refined approach significantly improves both the accuracy and practicality of the V-notch as a flow measurement instrument.

The stage-discharge relationship governing triangular cross-sections, such as those found in triangular weirs, is based on a well-established formula, widely acknowledged in the literature (Bos, 1989; Hager, 1986; Achour and Amara, 2021a; 2021b; 2022b; 2023b; Achour and De Lapray, 2023). This relationship is particularly relevant to the V-notch in question, which operates similarly to a contracted triangular weir without a crest height. Given that the V-notch's discharge is governed by a triangular cross-section at the outlet, the same stage-discharge equation applies. Consequently, the flow rate through the V-notch mirrors that of a triangular weir, with discharge directly linked to the upstream depth (h_1), and the flow characteristics remain consistent with the hydraulics of standard triangular weirs.

Furthermore, the equation remains valid as long as free-flow conditions are maintained at the notch, meaning that the flow is not subjected to submergence downstream. The governing equation is conventionally articulated as follows:

$$Q = \frac{8}{15} C_d\, m_2 \sqrt{2g}\; h_1^{5/2} \tag{22}$$

By contrasting Eqs. (21) and (22), the exact relationship for the discharge coefficient (C_d) of the V-notch under consideration can be derived as follows:

$$C_d = \frac{15}{16} h_1^{*\,-5/2} \tag{23}$$

The derived Eq. (23) is of significant importance, as it is solely dependent on the upstream relative flow depth h_1^*, which is intrinsically linked to the section reduction ratio ζ, as outlined in Eq. (19). This indicates that the discharge coefficient (C_d) can be expressed as a function of ζ, which, in turn, is determined solely by the side slopes m_1 and m_2, or b and T, as defined in Eq. (5). As a result, Eq. (23) simplifies the stage-discharge equation for the V-notch under consideration, establishing a direct relationship between the geometry and the discharge coefficient. Moreover, it can be inferred from both Eqs. (23) and (19) that, for a given installation with specified side slopes m_1 and m_2, or the geometric parameters b and T, the V-notch discharge coefficient (C_d) remains invariant, irrespective of variations in the upstream flow depth h_1. The discharge coefficient (C_d) is exclusively

a function of the section reduction ratio ζ, which is defined by Eq. (5) as $\zeta = m_2/m_1 = b/T$. This distinctive characteristic - namely, the invariance of the discharge coefficient (C_d) with respect to variations in upstream flow depth h_1 - was likewise observed in the study conducted by Achour and Amara (2022g), which focused on the sharp-edged width constriction employed as a flow measurement device. In their investigation, it was demonstrated that the discharge coefficient for this type of structure is solely a function of the contraction rate β, defined as $\beta = b/B$, where b represents the width of the rectangular notch opening, and B corresponds to the width of the rectangular approach channel. This finding is valid within the recommended range $0.15 \leq \beta \leq 0.45$. For a specified installation, the geometric parameters - namely the notch opening b and the approach channel width B - are predefined and precisely established.

Unlike traditional empirical models, the derived Eq. (23) ensures that the discharge coefficient (C_d) is grounded in theoretical derivations, rather than relying on experimental calibrations. The derived Eq. (23) guarantees that:

$$C_d = f\left(h_1^*\right) = f\left(\zeta\right) \tag{24}$$

As demonstrated in a previous section, dimensional analysis predicted this outcome, thereby confirming that it accurately identifies the dependence of (C_d) on ζ.

Fig. 5 depicts the variation of (C_d) with ζ, as derived from Eqs. (19) and (23), within the recommended range of $0.35 \leq \zeta \leq 0.50$.

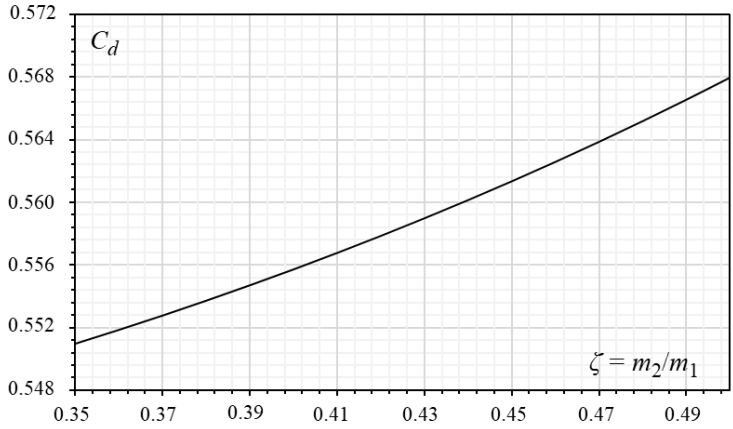

Figure 5: Variation of $C_d(\zeta)$ according to Eqs (19) and (23) within the recommended range $0.35 \leq \zeta \leq 0.50$

Fig. 5 illustrates that as ζ increases, the effect of flow contraction diminishes, resulting in a gradual rise in (C_d). It is important to remind the reader that the primary aim of this study is not to design a device that maximizes discharge capacity by increasing the discharge coefficient (C_d). Rather, the focus is on developing a device that facilitates the precise estimation of the flow rate conveyed through a given triangular open approach

channel. While Fig. 5 shows relatively high values of (C_d), these should not be construed as the central concern of the study. Elevated values of (C_d) are irrelevant to the research objectives and will not be discussed further. Maximizing (C_d) is distinct from optimizing flow measurement accuracy.

By substituting Eq. (20b) into Eq. (23), the following approximate governing relationship for the contracted V-notch discharge coefficient (C_d) is derived, resulting in a simplified yet precise expression for predicting (C_d) based on fundamental geometric parameters:

$$C_{d,appr} = \frac{15}{16}\left[0.291\left(1-\zeta^2\right)^{0.3521} + 0.959\right]^{-5/2} \tag{25}$$

where the subscript "*appr*" denotes "Approximate".

Within the established validity range of $0.35 \le \zeta \le 0.50$, the simplified Eq. (25) yields a maximal deviation of only 0.0005808% in the determination of the discharge coefficient (C_d) for the V-notch under consideration. This maximal deviation underscores the robustness and reliability of the approximate formulation, making it a highly practical alternative to the more complex exact expressions - namely, Eqs. (19) and (23) - which require iterative methods or trial-and-error procedures to obtain precise values of (C_d). This maximal deviation is inherently predicted by Eq. (23), as it allows the following relationship to be established:

$$\left(\frac{\Delta C_d}{C_d}\right)_{\max} = \frac{5}{2}\left(\frac{\Delta h_1^*}{h_1^*}\right)_{\max} = \frac{5}{2}\times 0.0002323 = 0.00058075\% \tag{26}$$

This level of predictability further reinforces the theoretical soundness and internal consistency of the proposed approximation. The newly derived formulation for the discharge coefficient (C_d) incorporates essential parameters, thereby enhancing both its accuracy and practical applicability. By simplifying the computational process, the approximate Eq. (25) significantly reduces analytical complexity, facilitating a more straightforward and efficient estimation of (C_d). This validation effectively dispels concerns regarding potential approximation errors, providing assurance that Eq. (25) can be applied with a high degree of confidence in engineering practice. Furthermore, if the predictions obtained from Eq. (25) exhibit strong agreement with experimental measurements, it will substantiate that the V-notch device operates within well-defined and predictable hydraulic limits. Nevertheless, it is recommended that the approximation be subjected to further evaluation under a variety of flow conditions to comprehensively verify its robustness and general applicability.

To enable readers a better appreciation of the deviations introduced by the approximate Eq. (25) in the computation of the discharge coefficient (C_d), within the recommended range $0.35 \le \zeta \le 0.50$, Table 1 has been specifically prepared for this purpose.

Table 1: Deviations introduced by the approximate Eq. (25) in the calculation of the crestless contracted V-notch discharge coefficient (C_d)

$\zeta = m_2/m_1 = b/T$	(C_d) Exact Eqs. (19) and (23)	(C_d) Approximate Eq. (25)	Deviation (%)
0.35	0.550959988	0.55096319	0.00058082
0.36	0.551845032	0.55184818	0.00057094
0.37	0.552762007	0.55276509	0.00055772
0.38	0.55371161	0.55371461	0.00054130
0.39	0.554694576	0.55469747	0.00052191
0.40	0.555711678	0.55571446	0.00049986
0.41	0.556763731	0.55676638	0.00047557
0.42	0,557851596	0.55785410	0.00044960
0.43	0.55897618	0.55897854	0.00042260
0.44	0.560138442	0.56014066	0.00039540
0.45	0.561339391	0.56134146	0.00036902
0.46	0.562580097	0.56258204	0.00034465
0.47	0.563861687	0.56386351	0.00032368
0.48	0.565185355	0.56518709	0.00030778
0.49	0.566552363	0.56655406	0.00029892
0.50	0.56796405	0.56796575	0.00029931

The following insights can be offered regarding the influence of employing the approximate Eq. (25) on the determination of the discharge coefficient (C_d). In particular, Table 1 presents the percentage deviations resulting from the application of this approximation within its established validity range, defined by $0.35 \leq \zeta \leq 0.50$.

Table 1 clearly demonstrates that the maximum deviation - amounting to just 0.00058082% - introduced by the use of the approximate Eq. (25) in the calculation of the discharge coefficient (C_d) occurs at the lowest bound of the section reduction ratio $\zeta = 0.35$. This exceptionally insignificant deviation underscores the high degree of reliability and precision associated with Eq. (25).

Consequently, engineers can apply this approximation with a high degree of confidence when estimating discharge in triangular open approach channels equipped with the proposed V-notch configuration, assured of its precision and free from concerns regarding significant computational inaccuracies or deviations from expected performance.

Theoretical framework grounded in the properties of the kinetic factor

The objective of this section is to propose an alternative approach for deriving the discharge coefficient (C_d) relationship for the V-notch under consideration, using the properties of the kinetic energy factor. This method serves as a verification pathway, aiming to reproduce the same theoretical result as that provided by the exact Eq. (23), albeit derived through a different analytical approach. By incorporating the kinetic factor into the dimensionless energy framework, this formulation offers an independent yet consistent validation of the theoretical discharge coefficient expression, reinforcing the robustness and coherence of the hydraulic model developed for the crestless contracted V-notch device in triangular open approach channels.

Eq. (14) can be reformulated in the following form:

$$h_1\left(1+\frac{Q^2}{2gm_1^2h_1^5}\right)=\frac{5}{4}h_{2,c} \tag{27}$$

The elimination of Q^2 between Eqs. (7) and (27) results in the following expression:

$$h_1\left(1+\frac{\frac{1}{2}gm_2^2h_{2,c}^5}{2gm_1^2h_1^5}\right)=\frac{5}{4}h_{2,c} \tag{28}$$

Upon performing straightforward simplifications, the following expression is derived:

$$h_1\left[1+\frac{\left(m_2/m_1\right)^2}{4\left(h_1/h_{2,c}\right)^5}\right]=\frac{5}{4}h_{2,c} \tag{29}$$

Since the ratios within the brackets of Eq. (29) have been clearly established earlier, the following expression can now be written:

$$h_1\left(1+\frac{\zeta^2}{4h_1^{*5}}\right)=\frac{5}{4}h_{2,c} \tag{30}$$

Eq. (30) may be rewritten in the following form:

$$h_1\left(1+\delta\right)=\frac{5}{4}h_{2,c} \tag{31}$$

where δ, referred to as the kinetic factor, is directly associated with the approach flow velocity and is defined by the following expression:

$$\delta = \frac{\zeta^2}{4h_1^{*5}} \tag{32}$$

The kinetic factor δ plays a fundamental role in hydraulic computations, as it accounts for the influence of flow velocity in the analysis of open channel hydraulics, thereby enhancing the accuracy of discharge estimations. A direct mathematical relationship can readily be established between δ and the mean approach flow velocity (V_1) in section 1-1 (Fig. 3), expressed as:

$$\delta = \left(\frac{V_1}{\sqrt{2gh_1}} \right)^2 \tag{33}$$

Furthermore, δ can be interpreted as the square of the velocity ratio between the actual approach velocity of the flow (V_1) and the theoretical velocity predicted by Torricelli's law. In this context, h_1 represents the vertical distance from the free surface of the upstream water level to the lowest point of the V-notch opening through which the liquid discharges. This interpretation underscores the physical significance of the kinetic factor δ, as it quantifies the deviation of actual flow conditions from idealized theoretical assumptions.

Eq. (32) demonstrates that the kinetic factor δ is solely governed by the section reduction ratio ζ, given that h_1^* is exclusively a function of ζ, as established by Eq. (19).

This relationship implies that all variations in the kinetic factor δ are directly attributable to changes in the section reduction ratio ζ. This finding is particularly significant for enhancing the understanding of velocity-related effects in hydraulic systems, as it underscores the role of ζ in governing the kinetic energy component of the flow.

Furthermore, computational analysis indicates that the kinetic factor δ consistently remains less than unity, varying within the range of $0.0106 \leq \delta \leq 0.0229$ as ζ varies within the recommended range $0.35 \leq \zeta \leq 0.50$. An increasing trend of δ with respect to ζ is observed, as highlighted in Table 2.

The rationale behind the increase of the kinetic factor δ as the section reduction ratio ζ increases can be readily demonstrated. The kinetic factor δ quantifies the contribution of the approach flow velocity to the total energy head in a hydraulic system. It is a dimensionless parameter representing the ratio between the kinetic energy of the actual flow and the potential energy head, normalized herein by h_1, the upstream flow depth.

Consider a given triangular open approach channel for which the value of m_1 or, equivalently, the top width T is known with certainty. As the section reduction ratio $\zeta = m_2/m_1 = b/T$ (Eq. 5) increases, the top width of the V-notch opening b becomes wider. While this reduces the degree of geometric constriction, it simultaneously affects the upstream flow depth h_1, which decreases with increasing b. The reduction in h_1 leads to an increase in the approach flow velocity V_1, according to the continuity equation, thereby elevating the kinetic energy component of the flow. As a result, the kinetic factor δ, which

quantifies the ratio of kinetic energy to potential energy head, increases with V_1, according to Eq. (33).

Although the kinetic factor δ consistently remains less than unity, its influence should not be disregarded in discharge calculations. Numerous flow measurement studies erroneously neglect the contribution of δ, which can result in significant inaccuracies - potentially leading to critical errors in the determination of the discharge coefficient (C_d). Overlooking δ effectively eliminates the consideration of approach flow velocity, thereby assuming that the associated kinetic energy component is negligible.

Table 2: Values of the kinetic factor (δ) corresponding to the recommended range of the section reduction ratio (ζ)

$\zeta = m_2/m_1$	δ
0.35	0.01057727
0.36	0.0112263
0.37	0.01189809
0.38	0.01259308
0.39	0.01331173
0.40	0.01405454
0.41	0.01482201
0.42	0.01561469
0.43	0.01643316
0.44	0.017278
0.45	0.01814987
0.46	0.01904942
0.47	0.01997737
0.48	0.02093446
0.49	0.02192147
0.50	0.02293925

Conversely, a decrease in the section reduction ratio ζ results in a corresponding decrease in both m_2 and the notch opening b, as established by Eq. (5). This reduction in b intensifies the geometric contraction effect imposed by the V-notch, thereby diminishing the cross-sectional area available for flow discharge. The immediate consequence of this increased constriction is a rise in the upstream water depth h_1, which, in turn, leads to a reduction in the approach flow velocity V_1, in accordance with the continuity equation. Following Eq. (33), the decrease in V_1, coupled with the increase in h_1, causes the kinetic factor δ to decline. As V_1 diminishes and h_1 becomes more dominant, the total upstream head H_1 effectively converges toward the static depth h_1, indicating that the contribution of the velocity head becomes negligible in comparison to the potential head.

Eliminating $h_{2,c}$ between Eqs. (11) and (31) yields the following:

$$\left(\frac{2Q^2}{g\,m_2^2}\right)^{1/5} = \frac{4}{5}\left(1+\delta\right)h_1 \tag{34}$$

This enables the discharge Q to be expressed in the following form:

$$Q = \frac{1}{2}\left(\frac{4}{5}\right)^{5/2}\left(1+\delta\right)^{5/2} m_2\sqrt{2g}\,h_1^{5/2} \tag{35}$$

Furthermore, a comparison between Eq. (22) and Eq. (35) leads to the derivation of the following relationship for the discharge coefficient (C_d):

$$C_d = C_0\left(1+\delta\right)^{5/2} \tag{36}$$

where C_0 represents a constant, which is defined as follows:

$$C_0 = \frac{15}{16}\left(\frac{4}{5}\right)^{5/2} \tag{37}$$

Based on Eqs. (32) and (36), the C_d discharge coefficient relationship can be expressed in the following final form:

$$C_d = C_0\left(1+\frac{\zeta^2}{4h_1^{*5}}\right)^{5/2} \tag{38}$$

where the relative upstream depth h_1^* can be accurately calculated using the approximate Eq. (20b). This confirms that (C_d) inherently includes kinetic energy effects, making the V-notch's discharge estimation more precise. Integrating the kinetic factor δ, ensures that velocity energy effects are naturally incorporated into the discharge formulation.

Moreover, as previously discussed, the kinetic factor δ cannot be disregarded in the analysis. According to Eq. (38), if δ were to be neglected, the discharge coefficient (C_d) would reduce to C_0, the constant value defined by Eq. (37). Such a simplification would lead to an erroneous result, as it fails to account for the influence of the approach flow velocity on (C_d), thereby compromising the accuracy of the discharge computation.

Eq. (38) presents the second formulation for the discharge coefficient (C_d) of the crestless contracted V-notch weir, derived by explicitly incorporating the influence of the kinetic factor δ. This expression provides further validation that (C_d) is exclusively determined by the dimensionless section reduction parameter ζ. Given that ζ is defined in terms of the side slopes coefficients m_1 and m_2, or b and T, as established by Eq. (5), the discharge coefficient exhibits an indirect dependency on these geometric parameters. This formulation reinforces the theoretical robustness of employing ζ as the principal governing variable in characterizing flow contraction effects through the V-notch, thereby simplifying the analytical description of the discharge process.

Although derived through two distinct methodological approaches, Eqs. (23) and (38) yield precisely identical results for the discharge coefficient (C_d), irrespective of the value of the section reduction parameter ζ. This consistency underscores the theoretical coherence and validity of both formulations across the entire range of ζ values.

EXPERIMENTAL VALIDATION OF THE THEORETICAL APPROACH FOR THE CRESTLESS V-NOTCH DISCHARGE COEFFICIENT

Detailed description of the test facility and device geometry

The experimental validation phase of the study is crucial for testing and refining the theoretical relationships previously developed. The main objective is to evaluate the accuracy of the approximate explicit Eq. (25), which governs the discharge coefficient (C_d) of the V-notch under consideration. The experiments test whether the theoretical predictions of (C_d) align with real-world measurements. If deviations exist between the predicted and observed (C_d) values, adjustments will be made to the constants in Eq. (25) to improve its accuracy. Recall that that (C_d) is exclusively influenced by the dimensionless section reduction ratio ζ, which consists of the side slopes $m_1$and m_2 of the V-notch, or the geometric parameters b and T as defined by Eq. (5).

Fig. 6 presents the hydraulic installation specifically engineered for the experimental investigation of flow measurement devices in open channel systems.

The experimental study ensures that flow conditions, measurement techniques, and data processing meet high experimental standards.

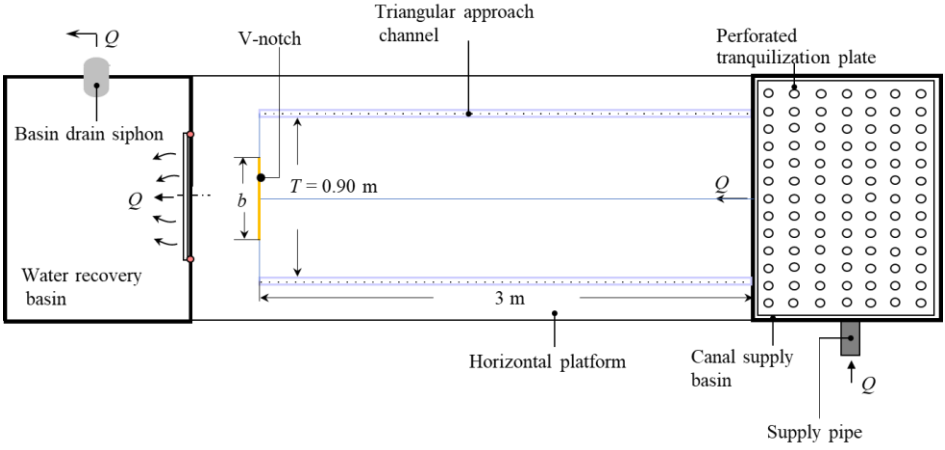

Figure 6: Prototype of the V-notch undergoing experimental evaluation on a custom-designed hydraulic platform (Dimensions not to scale)

The sidewalls of the triangular open approach channel are constructed from two precision-cut Plexiglas plates, each measuring 3 m in length and 1.5 cm in thickness. Using a specialized large digital caliper, the first plate has a width of 65.14 centimeters, while the second measures 63.64 centimeters in width. These plates are meticulously assembled to form an apex angle of 90°, ensuring geometric accuracy in accordance with the channel's design specifications. The selected apex angle of 90° corresponds to a side slope $m_1 = 1$.

To achieve a structurally sound and watertight joint, the plates are bonded along their entire contact interface using chloroform as a solvent welding agent. The chloroform is carefully and uniformly applied to the joint surfaces to facilitate the dissolution of the Plexiglas at the molecular level, since chloroform is known for its power to polymerize plexiglass, thereby creating a seamless and robust weld upon curing. This method guarantees an optimal hydraulic seal and a highly durable bond between the plates, both of which are essential to preserving the structural integrity and ensuring the reliable functionality of the approach channel throughout the experimental investigations. The precision and effectiveness of the bonding process are particularly critical for preventing leakage and maintaining controlled flow conditions, thereby upholding the accuracy and validity of the experimental results.

Following the completion of the final assembly of the approach channel walls and their placement on appropriately designed supports (Fig. 1), the top width T was precisely measured using a laser distance meter, and found to be 90 cm; this results in a channel depth $h_o = T/2$, yielding $h_o = 90/2 = 45$ cm. This calculation is consistent with Eq. (1b), considering that the side slope $m_1 = 1$, as previously noted.

The top width of the triangular open approach channel, $T = 90$ cm, provides sufficient breadth to facilitate the testing of a representative range of V-notch top widths b. In accordance with the established guidelines, the top width b is rigorously maintained within the recommended range of $0.35T$ to $0.50T$, corresponding to $31.5 \text{ cm} \leq b \leq 45$ cm. The measurement of the top width b is performed exclusively after the precise installation and secure fastening of the V-notch plates.

The two plates, denoted as ABCA and A'B'CA' in Fig. 2, which together form the V-notch under consideration, are individually designed and fabricated from a thin stainless-steel sheet with a thickness of only 1 mm. This minimal thickness was deliberately selected to eliminate any potential structural or hydraulic interference within the flow system. As previously described, these plates are securely affixed and sealed to the outlet section of the channel using rivets (Fig. 2). Additionally, a high-quality rubber gasket is adhesively bonded along the contact surface to ensure complete watertightness at the channel's exit section, thereby effectively preventing any leakage.

The experimental setup facilitated the testing of nine distinct V-notch configurations, each characterized by a different top width b, as detailed in Table 3. The Table 3 also consolidates the corresponding values of the top width T of the triangular open approach channel, along with the associated section reduction ratios ζ. Given that the side slope m_1

is equal to 1, the corresponding value of m_2 is consequently determined to be equivalent to the section reduction ratio ζ, in accordance with the relationship defined by Eq. (5).

The experimental values of ζ confirm that they fall within the validity range of the approximate theoretical Eq. (25). This ensures that the theoretical discharge coefficient model remains applicable to real-world conditions.

Table 3: Geometric properties of the tested crestless contracted V-notches including top widths (b), (T), and section reduction ratios ($\zeta = b / T = m_2$)

Device	b (m)	T (m)	$\zeta = m_2$
1	0.320	0.90	0.35555556
2	0.350	0.90	0.38888889
3	0.382	0.90	0.42444444
4	0.403	0.90	0.44777778
5	0.418	0.90	0.46444444
6	0.424	0.90	0.47111111
7	0.433	0.90	0.48111111
8	0.440	0.90	0.48888889
9	0.446	0.90	0.49555556

Description of the experimental hydraulic parameters

The experimental discharge coefficient, denoted as ($C_{d,\,Exp}$), is determined using Eq. (22), which offers a practical methodology for calculating (C_d) based on the measured discharge values obtained during testing. This formulation plays a pivotal role in the validation of the theoretical model, ensuring coherence between the computed predictions and the empirical observations. The value of ($C_{d,\,Exp}$) is derived from the experimental data collected through the hydraulic testing apparatus, facilitating a direct and meaningful comparison with the approximate theoretical discharge coefficient as defined by Eq. (25).

The resulting expression for ($C_{d,\,Exp}$) is given by the following:

$$C_{d,\,Exp} = \frac{15}{8} \frac{Q_{Exp}}{m_2 \sqrt{2g}\, h_{1,\,Exp}^{5/2}} \tag{39}$$

The nine values of the side slope m_2, corresponding to each of the tested V-notch configurations, are systematically presented in Table 3. The values of m_2 have been determined with such precision that they are not subject to any measurable error.

In order to ensure the reliability and validity of Eq. (39), which is employed to experimentally determine the discharge coefficient (C_d) of the V-notch, it is essential to evaluate both the experimental discharge (Q_{Exp}) and the upstream flow depth ($h_{1,\,Exp}$) with the highest degree of precision. Any inaccuracies in measuring these two fundamental

parameters can directly compromise the accuracy of the calculated discharge coefficient, and hence the discharge Q, leading to erroneous interpretations and undermining the validation of the theoretical model.

Precise determination of (Q_{Exp}) ensures that the actual flow rate through the V-notch is correctly quantified, which is critical for validating the theoretical discharge predictions. Likewise, accurate measurement of ($h_{1,\,Exp}$), representing the upstream water level, is imperative because even minor errors in depth readings can significantly distort the computation of the energy head and, consequently, the derived (C_d). The sensitivity of discharge measurements to upstream depth in open channel flow systems necessitates meticulous attention to data collection, particularly in maintaining steady-state flow conditions and minimizing experimental uncertainties.

Therefore, rigorous calibration of instrumentation and adherence to precise measurement protocols are indispensable to ensuring the integrity of the experimental validation process.

The experimental discharge, (Q_{Exp}), was not measured directly; rather, it was calculated as the average of the readings obtained from both an ultrasonic flow meter and a magnetic flow meter. Prior to testing, both instruments underwent meticulous calibration to ensure measurement accuracy and minimize potential errors. This methodology resulted in an absolute measurement error of only 0.1 L/s, thereby guaranteeing a high degree of precision in the determination of the flow rate.

Given that (Q_{Exp}) plays a critical role in the calculation of the experimental discharge coefficient ($C_{d,\,Exp}$), according to Eq. (39), the reduction of systematic errors in flow rate measurement significantly enhances the reliability and validity of the study's findings. Accurate estimation of (Q_{Exp}) is therefore essential to ensure the credibility of the experimental validation of the theoretical model.

The experimental upstream flow depth, ($h_{1,\,Exp}$), was measured using a double-precision Vernier point gauge, featuring graduations accurate to one-tenth of a millimeter (0.1 mm). The measurement process achieved an absolute error margin of only 0.02 mm. Considering that the minimum recorded upstream depth was 50 mm, this corresponds to a maximum relative deviation of merely 0.01%, as calculated by (50 × 0.02) / 100 = 0.01%. This relative error associated with the measurement of the upstream flow depth ($h_{1,\,Exp}$) results in a propagated relative error of 2.5 × 0.01 = 0.025% in the calculation of the discharge coefficient (C_d). This quantifies the sensitivity of (C_d) to measurement inaccuracies in ($h_{1,\,Exp}$), underscoring the importance of precision in depth readings to ensure reliable discharge coefficient determinations.

The double-precision Vernier point gauge utilized in this investigation was comprehensively described in a previous study by Achour and Amara (2022g).

In principle, according to the approximate Eq. (25), there exists a unique value of the discharge coefficient (C_d) corresponding to a given V-notch configuration, specifically characterized by a well-defined section reduction ratio ζ. This relationship holds

irrespective of variations in the upstream flow depth h_1, indicating that (C_d) remains constant for a fixed geometry defined by ζ.

However, this assertion remains theoretical, as experimental testing yields a distinct discharge coefficient ($C_{d,\,Exp}$) for each measured upstream flow depth ($h_{1,\,Exp}$), calculated in accordance with Eq. (39). Despite this variability, the experimentally determined ($C_{d,\,Exp}$) values exhibit minimal dispersion, remaining closely grouped. The final discharge coefficient ($C_{d,\,Exp}$) for the tested V-notch is established as the arithmetic mean of all the individual ($C_{d,\,Exp}$) values derived from Eq. (39). This averaged experimental discharge coefficient is subsequently compared with the approximate discharge coefficient ($C_{d,\,appr}$) predicted by Eq. (25). The close agreement between these two values serves to validate the theoretical approximate Eq. (25).

The hydraulic conditions implemented during the validation of the nine V-notch configurations facilitated the collection of approximately 2,879 data points, each corresponding to measured values of the experimental discharge (Q_{Exp}) and the upstream flow depth ($h_{1,\,Exp}$). A detailed compilation of these measurements, organized according to each tested device, is presented in Table 4. The acquisition of such a comprehensive dataset ensures that the validation of Eq. (25), which defines the discharge coefficient (C_d), is statistically robust and reliable. The extensive sample size not only enhances the credibility of the validation process but also allows for a thorough error analysis and the potential refinement of theoretical predictions, thereby strengthening the overall accuracy of the proposed model.

Table 4: Observed hydraulic parameters throughout the experimental tests of the nine V-notches

Device	Number of measures	Range of ($h_{1,\,Exp}$) (cm)	Range of (Q_{Exp}) (L/s)	(ζ_{Exp})
1	302	[5.02; 43.60]	[0.2614; 58.123]	0.35555556
2	325	[5.00; 44.20]	[0.2604; 60.502]	0.38888889
3	330	[5.10; 44.60]	[0.2753; 62.300]	0.42444444
4	332	[5.08; 44.10]	[0.2740; 60.861]	0.44777778
5	306	[5.20; 43.80]	[0.2918; 60.000]	0.46444444
6	312	[5.05; 44.00]	[0.2715; 60.823]	0.47111111
7	307	[5.00; 44.30]	[0.2655; 62.026]	0.48111111
8	328	[5.40; 44.20]	[0.3224; 61.786]	0.48888889
9	337	[5.30; 44.40]	[0.3083; 62.597]	0.49555556

Table 4 indicates that the experimental discharge (Q_{Exp}) and the upstream flow depth ($h_{1,\,Exp}$) were systematically varied across an extensive and practically relevant range, ensuring that the V-notch under consideration was rigorously evaluated under diverse flow conditions. Specifically, discharge measurements encompassed a broad interval from 0.2604 L/s to 62.597 L/s. This comprehensive range allowed for the assessment of

the device's performance under both low-flow and high-flow scenarios, thereby enhancing the applicability of the results to real-world hydraulic systems.

The wide variation in (Q_{Exp}) facilitated an in-depth evaluation of flow contraction effects across different discharge rates. Correspondingly, the resulting upstream flow depths ($h_{1,\ Exp}$) varied between 5.00 cm and 44.60 cm. Testing over this broad depth range was critical for verifying the validity and consistency of the approximate theoretical discharge coefficient Eq. (25) under varying approach flow conditions. This methodological approach strengthens the robustness of the experimental validation and confirms the model's suitability for a wide spectrum of hydraulic applications.

Experimental results and analysis

Table 5 consolidates the experimental data obtained from observations conducted on the nine V-notch configurations evaluated during the testing program.

Firstly, the experimental section reduction ratio ζ, assigned to each of the nine V-notch configurations tested, is presented alongside the corresponding discharge coefficients $C_{d,\ Appr}$ (ζ), which have been calculated using the approximate Eq. (25). The experimental validation aims to confirm the reliability and accuracy of this approximate formulation within the recommended range of ζ values.

For each series of experimental discharge values (Q_{Exp}) and upstream flow depths ($h_{1,\ Exp}$) reported in Table 4, the corresponding minimum (C_d min) and maximum (C_d max) discharge coefficients, calculated in accordance with Eq. (39), are presented in Table 5. The inclusion of these specific values is deliberate, as their close proximity to one another demonstrates the consistency and stability of the experimentally determined discharge coefficients ($C_{d,\ Exp}$). This minimal variation strongly suggests that all ($C_{d,\ Exp}$) values remain tightly clustered, irrespective of fluctuations in (Q_{Exp}) and ($h_{1,\ Exp}$), thereby reinforcing the reliability of the results.

For each series of experimental discharge measurements (Q_{Exp}) and corresponding upstream flow depths ($h_{1,\ Exp}$), the mean discharge coefficient ($C_{d,\ Exp}$) was computed and systematically reported in Table 5. The Table 5 also presents, for each of the nine V-notches tested, the deviations between the predicted discharge coefficients ($C_{d,\ Appr}$) calculated using the theoretical approximate Eq. (25), and the experimentally determined mean discharge coefficients.

It can therefore be observed that the maximum deviation introduced by the application of approximate Eq. (25) in the calculation of the V-notch discharge coefficient remains below 0.015%. This exceptionally low margin of error provides indisputable evidence of the accuracy and reliability of both Eqs. (25) and (22), affirming their suitability for confidently predicting the discharge coefficient (C_d) and the corresponding flow rate (Q), respectively. These findings are particularly relevant for triangular open approach channels employing the recommended V-notch configuration, which is specifically designed without a crest height.

Table 5: Experimental discharge coefficients for the nine tested V-notches and deviations associated with Eq. (25)

V-notch	ζ (Exp)	$C_{d,\,Appr}$ Eq. (25)	C_d (min)	C_d (max)	Mean C_d (Exp)	Deviation (%)
1	0.35555556	0.55145095	0.55136614	0.55144614	0.551402121	0.00885504
2	0.38888889	0.55458659	0.55458628	0.55478794	0.554568711	0.003224508
3	0.42444444	0.55834927	0.55833544	0.55839363	0.558324542	0.00442798
4	0.44777778	0.56107122	0.56101982	0.56106148	0.561024065	0.00840437
5	0.46444444	0.56314646	0.56307781	0.56321261	0.563175210	0.00510518
6	0.47111111	0.56400847	0.56396719	0.56400855	0.563928787	0.01412875
7	0.48111111	0.56533681	0.56533875	0.56537257	0.565335566	0.0002205
8	0.48888889	0.56639999	0.56634191	0.56644132	0.566316162	0.01479994
9	0.49555556	0.56733272	0.56733606	0.56739729	0.567346668	0.00245858
						Max. 0.01479994%

To further substantiate this compelling result, Fig. 7 has been prepared. It clearly demonstrates, if additional confirmation were needed, that the theoretical discharge coefficients predicted by the approximate Eq. (25) - illustrated by the solid line - exhibit exceptional agreement with the experimentally determined values, which are represented by the data markers. This alignment underscores the validity and reliability of the theoretical model across the range of conditions tested.

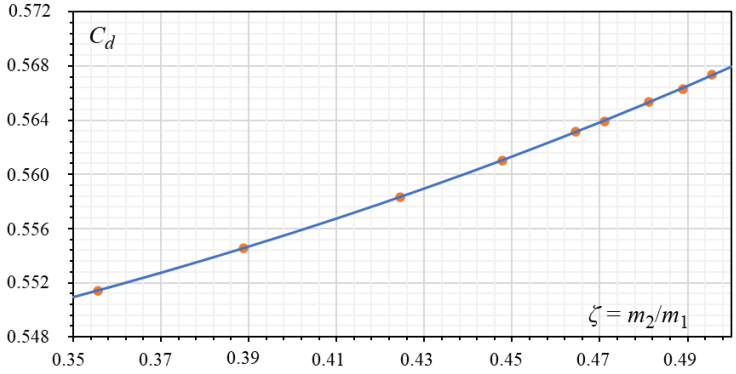

Figure 7: Variation of the discharge coefficients for the tested crestless contracted V-notches. (—) Predicted values based on Eq. (25); (●) Experimental observations

The outstanding results achieved in the evaluation of the V-notch are primarily attributable to the application of a rigorous theoretical framework, coupled with the acquisition of high-quality experimental data obtained through the use of precision instrumentation. This combination of robust analytical modeling and meticulous measurement techniques has ensured the accuracy and reliability of the findings.

CONCLUSION

This study has developed and rigorously validated a new theoretical framework for predicting the discharge coefficient (C_d) of a contracted V-notch installed at the downstream end of a triangular open approach channel. Grounded in energy principles and reinforced through dimensional analysis, the proposed model introduces a discharge coefficient formulation that is uniquely dependent on the dimensionless section reduction ratio (ζ), representing the geometric contraction imposed by the V-notch relative to the triangular open approach channel.

Two distinct theoretical methodologies—one based on the dimensionless energy equation and the other on the properties of the kinetic factor (δ) - have independently yielded consistent formulations for the discharge coefficient. The equivalence of these approaches confirms the theoretical soundness and internal consistency of the derived expressions. Notably, the discharge coefficient (C_d) demonstrated invariance with respect to the upstream flow depth (h_1), affirming its exclusive dependency on the geometric parameter ζ. This remarkable characteristic enhances the practicality of the proposed V-notch configuration as a reliable flow measurement device.

To complement the theoretical development, an extensive experimental campaign was conducted on nine distinct V-notch configurations, covering a wide and representative range of section reduction ratios ($0.35 \leq \zeta \leq 0.50$). Over 2,879 data points were collected, encompassing a broad spectrum of discharge rates and upstream flow depths. The experimental discharge coefficients ($C_{d,\ Exp}$) obtained from these tests exhibited exceptional agreement with the theoretical predictions derived from the approximate explicit Eq. (25), with a maximum deviation not exceeding 0.015%. This negligible discrepancy confirms the validity, robustness, and predictive accuracy of the theoretical model under practical flow conditions.

The study also emphasized the importance of high-precision instrumentation and strict adherence to calibration procedures in minimizing experimental uncertainties. The accuracy of upstream depth ($h_{1,\ Exp}$) measurements, facilitated by a double-precision Vernier point gauge, and the precise determination of discharge (Q_{Exp}) using both ultrasonic and magnetic flow meters, were critical in ensuring the reliability of the validation process.

The findings demonstrate that the proposed V-notch, devoid of crest height and installed in a triangular open approach channel, serves as an efficient and accurate flow measurement device. Its simple geometric design, ease of implementation, and self-cleaning capability make it particularly suited for field applications in irrigation systems, water distribution networks, and environmental monitoring programs.

Future research should explore the development and evaluation of alternative cost-effective methodologies for accurately measuring flow rates in triangular open channels. Emphasis should be placed on designing simple, reliable, and easily deployable solutions that maintain high levels of precision while minimizing construction and operational costs. Nevertheless, the present study provides a practical, theoretically robust, and

experimentally validated methodology for accurately measuring discharge in open channels with a triangular cross-sectional profile, for which the available weirs and flumes are not suitable.

MAIN RESULTS OF THE STUDY

This comprehensive study on the application of the crestless V-notch as an efficient flow measurement device in triangular open approach channels has produced a number of critical insights and key findings, detailed as follows:

Development of a theoretical model for the discharge coefficient (C_d)

The study presents a comprehensive theoretical formulation governing the discharge coefficient (C_d) of a contracted V-notch installed at the downstream end of a triangular open channel. Two distinct theoretical approaches were applied - one based on the dimensionless energy equation and another relying on the properties of the kinetic factor (δ). Both methods yielded identical and consistent results, confirming the robustness of the theoretical model.

Discharge coefficient (C_d) exclusively dependent on the section reduction ratio (ζ)

The analysis demonstrates that the discharge coefficient (C_d) depends solely on the section reduction ratio, defined as $\zeta = m_2 / m_1 = b / T$, where m_1 and m_2 are the side slopes of the triangular open approach channel and the V-notch, respectively, and b and T are the top widths of the V-notch and the channel. (C_d) is independent of the upstream flow depth (h_1), making it a reliable and geometry-governed parameter.

Proposal of an explicit (C_d) approximate equation (Eq. 25)

An explicit, simplified approximation for (C_d) (Eq. 25) was derived to facilitate practical engineering applications. This equation provides highly accurate results while significantly reducing computational complexity. The maximum deviation of (C_d) values computed using Eq. (25), relative to the exact values, was found to be less than 0.000581%, providing clear evidence of the exceptional accuracy of Eq. (25).

Experimental validation of the theoretical model

An extensive experimental campaign was conducted on nine distinct V-notch configurations, covering section reduction ratios in the range $0.35 \leq \zeta \leq 0.50$. The experimental dataset included 2,879 measurement points of discharge (Q_{Exp}) and upstream flow depth ($h_{1,\,Exp}$). The average experimental discharge coefficients ($C_{d,\,Exp}$) closely matched the theoretical predictions from Eq. (25), with deviations not exceeding 0.015 %.

Accuracy of experimental measurements

The upstream flow depth ($h_{1,\ Exp}$) was measured with high precision using a double-precision Vernier point gauge with an absolute error of 0.02 mm. Discharge (Q_{Exp}) was calculated as the average of readings from calibrated ultrasonic and magnetic flow meters, with an absolute error of 0.1 L/s. These rigorous measurement protocols ensured the reliability of the experimental validation.

Confirmation of (C_d) invariance with h_1

The experimental data confirmed the theoretical prediction that the discharge coefficient (C_d) remains constant for a given section reduction ratio ζ, independent of the upstream flow depth (h_1). This characteristic simplifies flow measurement since a single (C_d) value can be used for each V-notch configuration.

Practical advantages of the advocated crestless V-notch device

The crestless contracted V-notch is simple to construct, does not require a crest height, and is self-cleaning, minimizing sediment accumulation at the notch entrance. Its design enables precise discharge measurement in triangular open channels, particularly in irrigation and water distribution systems.

Declaration of competing interest

The authors declare that they have no known competing financial interests or personal relationships that could have appeared to influence the work reported in this paper.

REFERENCES

ACHOUR B. (1989). Jump flow meter in a triangular cross-section without weir, Journal of Hydraulic Research (In French), Vol, 27, Issue 2, pp, 205-214.

ACHOUR B., BOUZIANE M.T., NEBBAR M.L. (2003). Triangular broad crested flowmeter in a rectangular channel, Larhyss Journal, No 2, pp. 7-43. (In French)

ACHOUR B., AMARA L. (2020). Discussion of "discharge coefficient of shaft spillway under small heads, by Gouryev A.P., Brakeni A., Beglarova E.C., Larhyss Journal, No 43, pp. 7-11.

ACHOUR B., AMARA L. (2021a). Discharge coefficient for a triangular notch weir-theory and experimental analysis, Larhyss Journal, No 46, pp. 7-19.

ACHOUR B., AMARA L. (2021b). Theoretical discharge coefficient relationship for contracted and suppressed rectangular weirs, Larhyss Journal, No 45, pp. 165-182.

ACHOUR B., AMARA L. (2021c). Discharge coefficient of a parabolic weir, theory and experimental analysis, Larhyss Journal, No 46, pp. 77-88.

ACHOUR B., AMARA L. (2021e). Theoretical discharge coefficient relationship for a contracted triangular notch weir, experimental analysis for the special case of the 90-degree V-notch, Larhyss Journal, No 46, pp. 89-100.

ACHOUR B., AMARA L. (2021f). Discharge measurement in a rectangular open-channel using a sharp-edged width constriction - theory and experimental validation, Larhyss Journal, No 45, pp. 141-163.

ACHOUR B., AMARA L., MEHTA D. (2022a). Control of the hydraulic jump by a thin-crested sill in a rectangular channel, new experimental considerations, Larhyss Journal, No 50, pp. 31-48.

ACHOUR B., AMARA L. (2022b). Triangular broad crested weir, theory and experiment, Larhyss Journal, No 49, pp. 37-66.

ACHOUR B., AMARA L., MEHTA D., BALAGANESAN P. (2022c). Compactness of Hydraulic Jump Rectangular Stilling Basins Using a Broad-Crested Sill, Larhyss Journal, No 51, pp. 31-41.

ACHOUR B., AMARA L., MEHTA D. (2022d). New theoretical considerations on the gradually varied flow in a triangular channel, Larhyss Journal, No 50, pp. 7-29.

ACHOUR B., AMARA L. (2022e). Rectangular broad-crested flow meter with lateral contraction - theory and experiment, Larhyss Journal, No 49, pp. 85-122.

ACHOUR B., AMARA L. (2022f). Accurate discharge coefficient relationship for the Crump weir, Larhyss Journal, No 52, pp. 93-115.

ACHOUR B., AMARA L. (2022g). Discharge coefficient relationship for the sharp-edged width constriction new theory and experiment, Flow Measurement and Instrumentation, Vol. 88, Paper ID 102269.

ACHOUR B., AMARA L. (2023a). Control of the hydraulic Jump by a broad-crested sill in a rectangular channel - new theory and experiment, Larhyss journal, No 54, pp.145-174.

ACHOUR B., DE LAPRAY G. (2023). Curved Wall Triangular Flume (CWTF), Design, Theory, and Experiment, Larhyss Journal, No 56, pp. 139-178.

ACHOUR B., AMARA L, (2023b), The 2A triangular weir, Design, Theory and Experiment, Larhyss Journal, No 55, pp, 191-213,

ACHOUR B., AMARA L., KULKARNI K.H. (2024). Modified Montana Flume (MMF), Larhyss Journal, No 60, pp. 55-85.

ACHOUR B., MEHTA D., AZAMATHULLA H.M. (2024). A new trapezoidal flume for open channel flow measurement - design, theory, and experiment, Larhyss Journal, No 59, pp. 157-179.

ACHOUR B., AMARA L., KULKARNI K.H. (2025a). In-depth Investigation of Flow Measurement Using Sharp-edged Width Constriction in Trapezoidal Open Channels, Larhyss Journal, No 62, pp. 7-35.

ACHOUR B., AMARA L., KULKARNI K.H. (2025b). Development and validation of a modified H-flume for accurate flow measurement in rectangular channels, Larhyss Journal, No 61, pp. 241-286.

AFBLB (Financial agency of the Loire and Brittany basin). (1970). Book of special requirements for the production and approval of devices for measuring the flow of effluents. (In French)

AMARA L., ACHOUR B. (2021), Theoretical approach to stage-discharge relationship for a circular sharp-crested weir, Larhyss Journal, No 46, pp. 101-113.

BAZIN H. (1898). New experiments on Weir flow, Dunod Editions, Paris, France. (In French)

BOS M.G. (1989). Discharge measurement structure, 3rd Edition, Publication 20, International Institute for Land Reclamation and Improvement, Wageningen, Netherlands.

BOS M.G. (1976). Discharge measurement structures, hydraulic laboratory, Wageningen, The Netherlands, Report 4, May.

BRAKENSIEK D., OSBORN H., RAWLS W. (1979). Field manual for research in agricultural hydrology, agriculture handbook No 224, United Department of Agriculture, February, USA.

BRANDES D., BARLOW W.T. (2012). New Method for Modeling Thin-Walled Orifice Flow Under Partially Submerged Conditions, Journal of Irrigation and Drainage Engineering, Vol. 138, Issue 10, pp. 924-928.

CHOW V.T. (1959). Open Channel Hydraulics, McGraw-Hill, New York, USA.

DE COURSEY D.E., BLANCHARD B.J. (1970). Flow analysis over large triangular weir, Proceeding ASCE, Journal of Hydraulics Division, Vol, 96, HY7, pp. 1435-1454.

DEY S. (2002), Free overall in open channels: state-of-the-art review, Flow Measurement and Instrumentation, Vol. 13, Issues 5-6, pp. 247-264.

DISKIN M. (1961). The end depth at a drop in trapezoidal channel, Journal of Hydraulic Engineering, American Society of Civil Engineers, ASCE, Vol, 87, Issue 4, pp. 11-32.

FERRO V. (1999). Theoretical end-depth-discharge relationship for free overfall, Journal of Irrigation and Drainage Engineering, American Society of Civil Engineers, ASCE, Vol. 125, Issue 1, Technical Note No 15814.

FARZAD A., VATANKHAH A.R. (2023). Experimental study of simple flumes with trapezoidal contraction, Flow Measurement and Instrumentation, Vol, 90, Paper ID 102328.

GWINN W., PARSONS D. (1976). Discharge Equations for HS, H, and HL Flumes, Journal of the Hydraulics Division, Vol. 102, No 1.

GWINN W. (1984). Chute Entrances for HS, H, and HL Flumes, Journal of Hydraulic Engineering, May.

HAGER W.H. (1983). Hydraulics of plane free overfall, Journal of Hydraulic Engineering, American Society of Civil Engineers, ASCE, Vol. 109, Issue 12, pp. 1683-1697.

HAGER W.H. (1986). Discharge Measurement Structures, Communication 1, Department of Civil Engineering, Federal Polytechnic School of Lausanne, Switzerland. (In French)

KINDSVATER C.E., CARTER R.W. (1957). Discharge characteristics of rectangular thin-plate weirs, Proceeding ASCE, Journal of Hydraulics Division, Vol, 83, HY6, pp. 1453/1-6,

KULKARNI K.H., HINGE G.A. (2021). Performance enhancement in discharge measurement by compound broad crested weir with additive manufacturing, Larhyss Journal, No 48, pp. 169-188.

KULKARNI K.H., HINGE G.A. (2023). An energy perspective of composite broad crested weir for measuring accurate discharge, Larhyss Journal, No 54, pp. 85-106.

LANGHAAR H.L. (1962). Dimensional Analysis and Theory of Models, Wiley and Sons Inc.

MUHSIN K.A., NOORI B.M.A. (2021). Hydraulics of free overfall in smooth triangular channels, Ain Shams Engineering Journal, Vol. 12, Issue 3, pp. 2471-2484.

NABAVI S.V., ZEIGHAMI E., MIRHOSSEINI S.M. (2024). Free overfall in triangular channels – A review, Flow Measurement and Instrumentation, Vol, 97, Paper ID 102565.

OPEN CHANNEL FLOW., (2024). Brochures, Flow Tables, Instructions for Flumes, Manholes, Shelters, and Weirs, Atlanta, USA, Website accessible at https://www.openchannelflow.com/support/downloads-center

PARSHALL R.L. (1936). The improved Venturi flumes, Transaction, American Society of Civil Engineers, ASCE, Vol. 89, pp. 841–880.

RAJARATNAM N., MURALIDHAR D. (1964). End depth for exponential channels, Journal of Irrigation and Drainage Engineering, American Society of Civil Engineers, ASCE, Vol. 90, pp. 17-36.

ROUSE H. (1949), Engineering Hydraulics, Wiley, New York, USA.

SIA (Swiss Society of Engineers and Architects). (1936). Contribution to the study of gauging methods, Bulletin 18, Schweizer Wasserforschung, Bern, Switzerland. (In French)

VATANKHAH A.R., BIJANKHAN M. (2013). Discussion of New Method for Modeling Thin-Walled Orifice Flow Under Partially Submerged Conditions, Journal of Irrigation and Drainage Engineering, Vol.139, Issue 9, pp. 789-793.

ZUIKOV A.L. (2017). Hydraulics of the classical Crump weir water gauge, Power Technology and Engineering, Vol. 50, Issue 6, pp. 50-59.

APPENDIX

Perturbation solution for the implicit equation in h_1^*

Eq. (19), which implicitly governs the relative upstream flow depth $h_1{}^*(\zeta)$, is herein renumbered as Eq. (A1), where A denotes "Appendix". Thus:

$$h_1^{*5} - \frac{5}{4} h_1^{*4} + \frac{1}{4}\zeta^2 = 0 \tag{A1}$$

The exact solution can be expressed as an infinite series expansion truncated to a suitable order depending on the degree of accuracy required for the purpose.
The use of the perturbation method is used to derive the explicit analytical expression of $h_1{}^*(\zeta)$. To this end, let us introduce a perturbation parameter ε in Eq. (A1) leading to the following relationship:

$$h_1^{*5} - \frac{5}{4} h_1^{*4} + \frac{1}{4}\varepsilon\zeta^2 = 0 \tag{A2}$$

when $\varepsilon = 0$, the solution is straightforward, and $h_1{}^* = 5/4$. Surrounding this unperturbed solution, the analytical expression for $h_1{}^*$is subsequently given by:

$$h_1^* = h_{1(0)}^* + \varepsilon h_{1(1)}^* + \varepsilon^2 h_{1(2)}^* + \varepsilon^3 h_{1(3)}^* + \ldots \tag{A3}$$

Eq. (A3) can be rewritten if the following compact form:

$$h_1^* = \sum_{n=0}^{\infty} \varepsilon^n h_{1(n)}^* \tag{A4}$$

where $h_{1(n)}{}^*$ denotes the n-th order coefficient term solution of the perturbation series. By substituting Eq. (A4) into Eq. (A2), expanding it in Taylor series, and collecting terms in same order in ε, the coefficients $h_{1(n)}{}^*$ can be determined sequentially, as follows:

$$h_{1(0)}^* = \frac{5}{4};\ h_{1(1)}^* = -\left(\frac{8}{25}\right)^2 \zeta^2;\ h_{1(2)}^* = -\frac{1}{5}\left(\frac{16}{25}\right)^4 \zeta^4;$$

$$h_{1(3)}^* = -\frac{13}{50}\left(\frac{32}{50}\right)^6 \zeta^6 \tag{A5}$$

…and similarly for higher orders. It is important to note that the zero-th order solution corresponds to the unperturbed solution, i.e., $\varepsilon = 0$. By substituting the results from Eq. (A5) into Eq. (A4) and setting $\varepsilon = 1$, the perturbation solution up to the fourth order is expressed as follows:

$$h_1^* = \frac{5}{4} - \left(\frac{8}{25}\right)^2 \zeta^2 - \frac{1}{5}\left(\frac{16}{25}\right)^4 \zeta^4 - \frac{13}{50}\left(\frac{32}{50}\right)^6 \zeta^6 - \frac{51}{125}\left(\frac{32}{50}\right)^8 \zeta^8 \quad \text{(A6)}$$